Edinburgh Wave Power Project

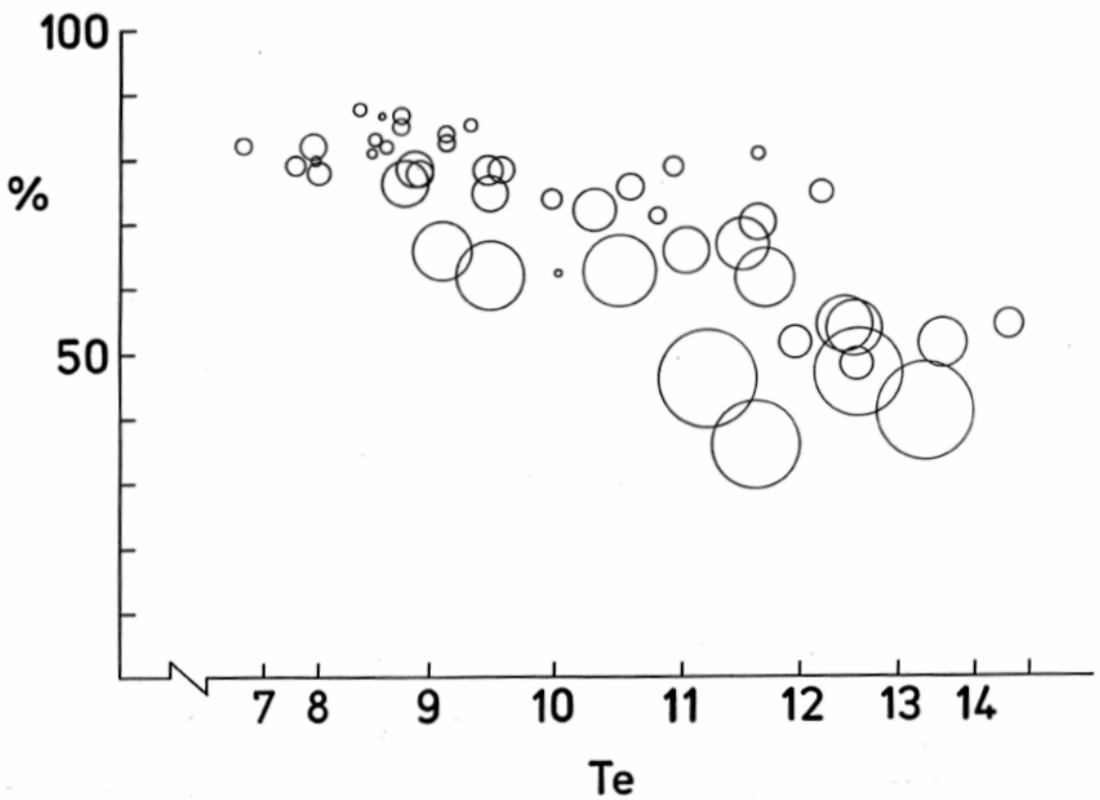

March 1985

VARIABLE COEFFICIENT CONTROL OF A WAVE-ENERGY DEVICE

H. E. YOUNG

J. POLLOCK

Introduction

In 1973 the optimisation of a duck was very quick; the mounting was rigidly fixed and the only variable control was the nod damping coefficient. The best setting could be discovered in a few minutes.

The 1974 designs allowed the variation of moment of inertia and changes to the position of the centre of gravity by variable ballast weights. A new model could be optimised in a few hours.

In 1975 it was found that phase-control of the nod-torque command could improve efficiency and widen bandwidth. This had the effect of adding negative spring and negative inertia. Duck optimisation took about two days.

In 1976 the group built a pitch-heave-surge rig shown opposite (Figure 1) which allowed the spring damping and inertia of two axes of the mounting to be separately controlled.

In 1977 a systematic sweep of the compliance domain revealed two areas of efficient operation which were separated by 'Death Valley' where an intermediate setting of heave compliance reduced duck nodding to virtually zero. It was found that reduced stiffness could double duck efficiency in long waves. But about three weeks of testing were necessary to determine the values for a range of frequencies.

In 1979 Mynett, Serman and Mei[1] produced a set of computer programmes which allowed the prediction of the hydrodynamic performance of an arbitrary shape on linear assumptions. Using their programs Greenhow simulated the behaviour of ducks on compliant mountings and came up with the conclusion that *any* shape could produce nearly 100% in a narrow tank provided that all three axes were properly controlled and that conditions remained linear.

At the same time work was being done in Edinburgh to explore the effects of power extraction from the model mounting using heave and surge damping in addition to heave and surge spring. It was also necessary to consider the effects of torque and force limits dictated by economic and structural requirements and this non-linearity took the problem beyond anything that could be handled by the theoretical workers. The combinatorial explosion of variables made experiments very tedious and led to the approach described in this paper.

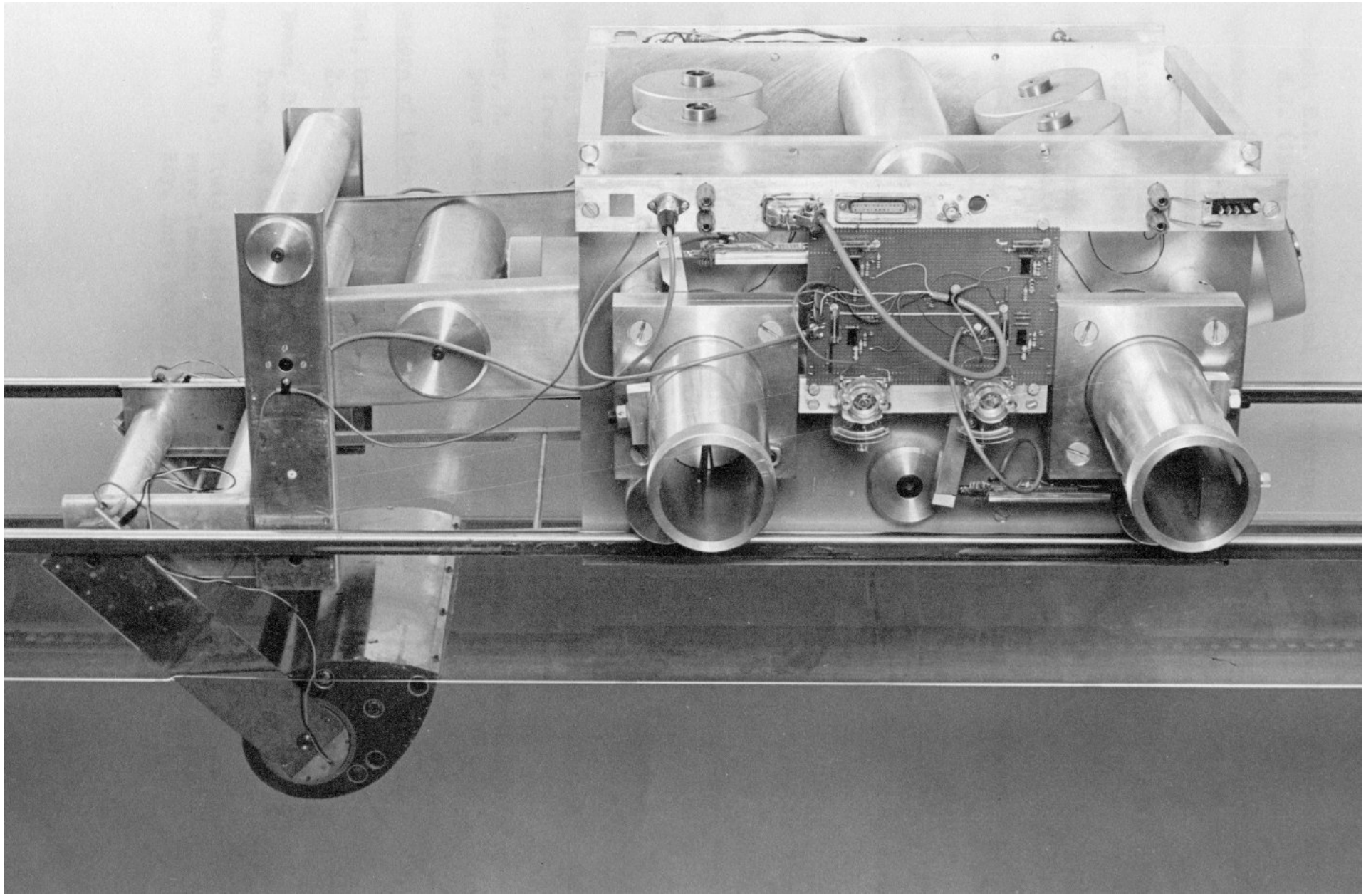

Figure 1

Apparatus and Experimental Procedure

Duck D0027 was mounted on the pitch-heave-surge rig in the Narrow Tank. Its width is 76% that of the tank, equivalent to the duck width-to-pitch ratio of the full-scale spine-mounted design. All efficiency calculations are based on the power in the entire width. The model scale is 1:140.

The test seas are uni-directional Pierson-Moskowitz (PM)[2] equivalents of the 46 spectra[3],[4], having the same statistical parameters (Te and Hrms). The wavemaking system consisted of an absorbing wavemaker driven by a modified PET microcomputer. The amplitude of the wavemaker drive signal was adjusted to produce the correct Hrms value by manual potentiometer settings for each individual sea. This corrected for random errors caused by the short length of a test run (90s at tank scale, 17.7 minutes at full scale).

The pitch-heave-surge rig[5] allows a duck to move in its three degrees of freedom. Transducers mounted on the rig measure velocity and force in the heave and surge modes. Nod angular velocity is measured and torque controlled by transducers mounted inside the duck. Displacement and acceleration signals are obtained by integrating and differentiating each velocity signal using conventional analogue computing techniques. Spring and damping in each mode can be simulated by multiplying the measured displacement and velocity signals by spring and damping coefficients, summing the two force components in each mode, and using the resulting signals to drive motors mounted on the rig.

During the first optimisation experiments,[6],[7] the spring and damping coefficients were varied manually by adjusting potentiometer settings. However, in this series of experiments digital computing techniques were used, and the coefficients were varied automatically under the control of two computers. More details of the apparatus are given in Appendix A.

Computer control offers two advantages. Firstly, the system controller (a Sirius microcomputer) can easily decide on the optimisation strategy and download different coefficients to the slave duck controller (PET microcomputer). Secondly, it is easy to use non-linear power take-off strategies since the duck controller can calculate any drive signal, given

its functional dependence upon the three sets of velocities and displacements.

It was initially thought that about 20 coefficients (eg squared spring and damping terms, displacement-dependent damping, cross products between the three modes, etc.) would prove useful. However, in this series of experiments, only seven were used in order to achieve a reasonably fast optimisation rate. These were spring and damping in each of the three modes, and the product of nod angle and nod velocity. The last coefficient results in a non-linear term in the power take-off strategy, and was included to allow the duck to have damping linearly dependent upon angular displacement (or spring linearly dependent upon angular velocity). The justification for this is that, as the angular displacement of the duck changes, the damping due to water changes, and it might be advantageous to either cancel or exaggerate this effect.

Thus the power take-off strategy used may be summarised by the following set of equations:-

$$H_D = HSC \times H + HDC \times \dot{H}$$

$$S_D = SSC \times H + SDC \times \dot{S}$$

$$\tau_D = DSC \times \theta + DDC \times \dot{\theta} + VDC \times \theta \times \dot{\theta}$$

where H_D = Heave drive

S_D = Surge drive

τ_D = Torque (duck) drive

and the coefficients are labelled in such a way that the first letter refers to the mode (Heave, Surge or Nod), the second letter refers to the coefficient type (Spring or Damping), and the last letter stands for coefficient. The seventh coefficient (VDC) is the Velocity times Displacement Coefficient.

The initial values of the six spring and damping coefficients were taken from the previous series of manually optimised experiments, and an approximate initial value for the seventh (VDC) was estimated from a series of preliminary experiments. A torque limit of 0.056 Nm (21.5 MNm at full scale) was applied to the nod drive signal, and a force limit of 3N (8.2 MN at full scale) was applied to the heave and surge drive signals. No power limit was applied, but it should be borne in mind that the present proposed mean power limit at full scale is 63 kW/m. In general, the only productivity limits which ought to be recognised are those imposed by swept volume, torque, mounting force and power rating.

The optimisation strategy was as follows. Small changes were made to each coefficient. If a change degraded the duck's performance it was rejected and the old value of the coefficient was restored. If, however, a change improved the performance, it was kept, and another similar change to the same coefficient in the same direction was tried. The criterion for an improvement in performance was that the sum of the power extracted from the three modes averaged over the 90 second test run should increase.

In addition to force and velocity measurements from the rig, the Sirius also recorded the waves in front of and behind the model with heaving float wavegauges. It transpired that there was a small but systematic rise in wave amplitude as an experiment proceeded. This was caused by tank evaporation, which reduces the tank depth by about 0.2% over a 12 hour period. Figures 2(a) and 2(b) show the effect of a finite tank depth on the wavelength. It can be seen that at low frequency, where most of the power in a sea is concentrated, a decrease in tank depth results in a decrease in wavelength, which in turn results in an increase in wave height, since wave period and energy must remain constant. This effect is also shown in Figure 3, where the ratio of deep to shallow water wave heights with constant power is plotted against Te for PM and monochromatic seas. These curves may be obtained by equating the deep water and depth corrected expressions for power due to Evans[8].

The overall result is a 2% rise in wave height over a 12 hour period in a typical PM sea. In order to compensate for this effect, all results were corrected by repeating several test runs with the original and final values of control coefficients after each optimistion had been completed.

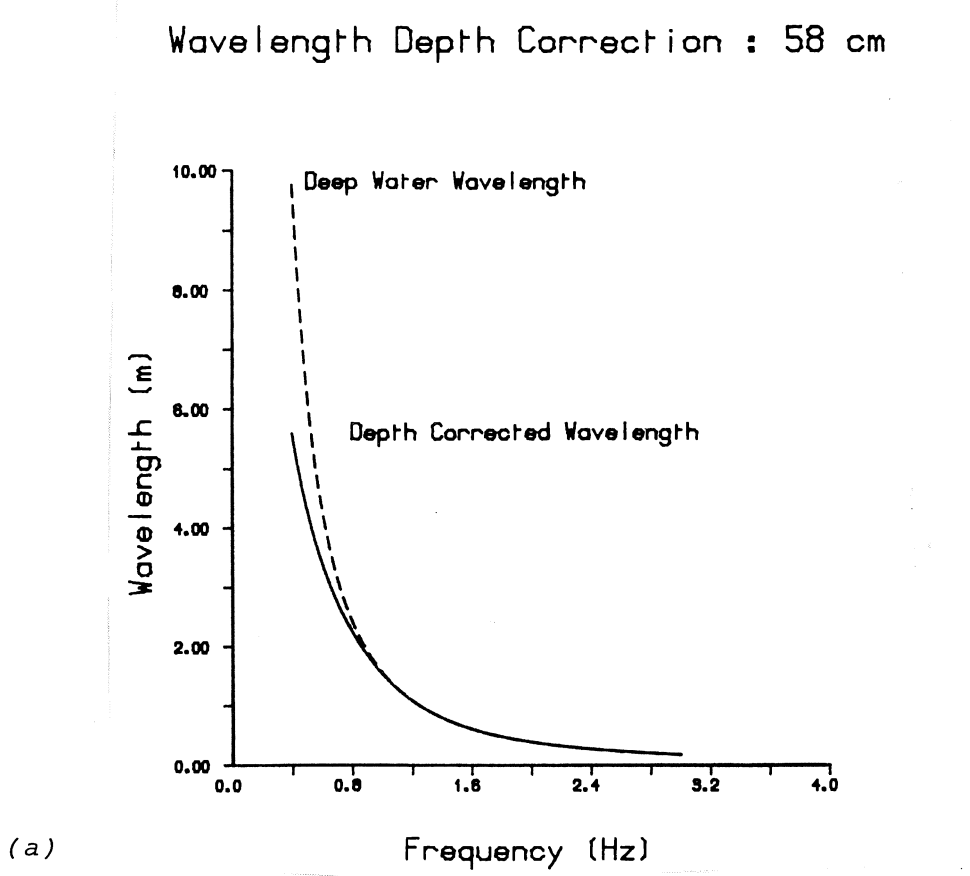

(a)

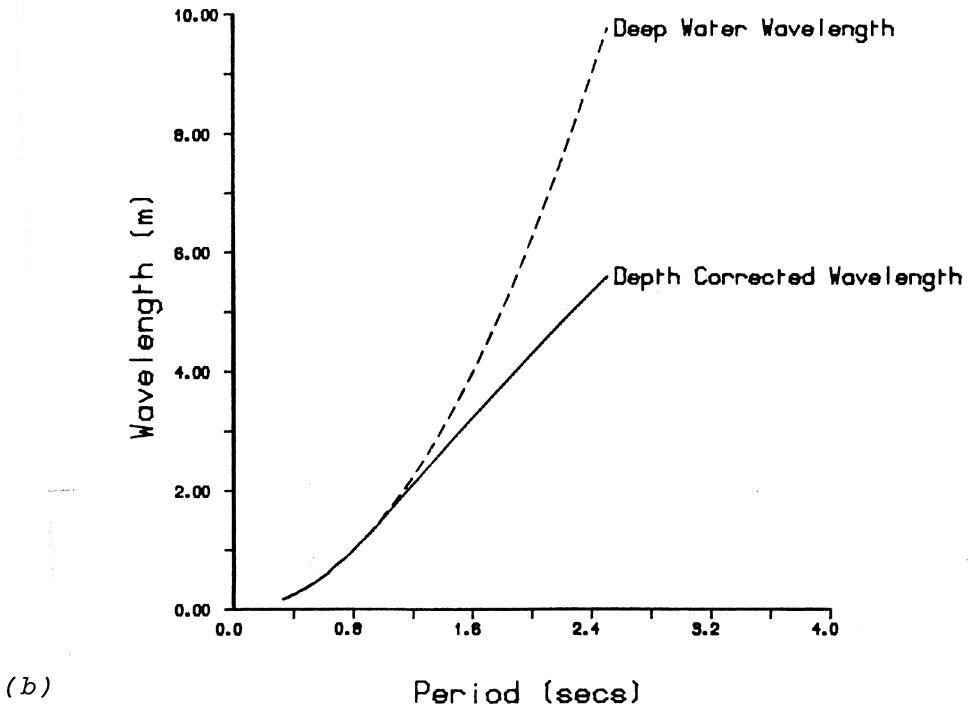

(b)

Figure 2: Deep water and depth corrected wavelengths vs. (a) frequency and (b) period.

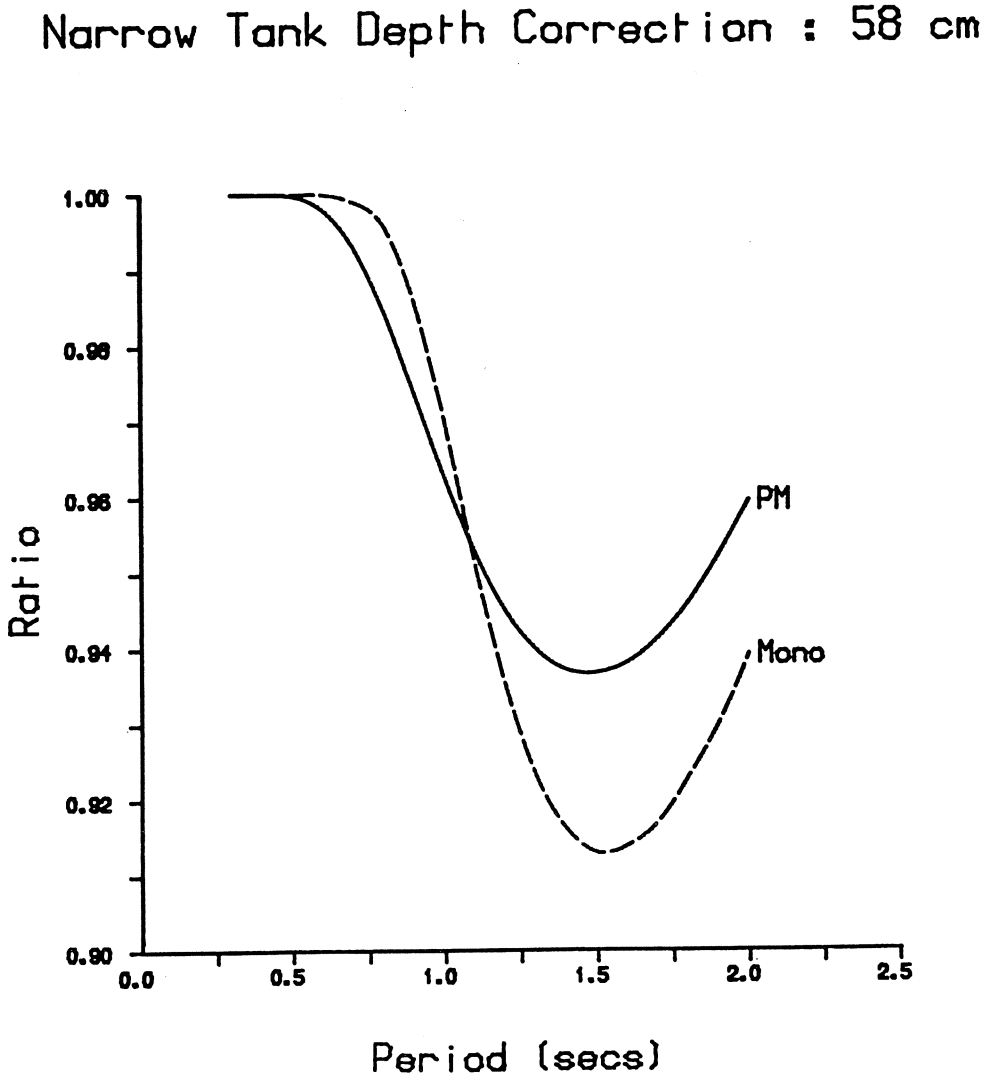

Figure 3: Ratio of deep to shallow water wave heights with constant power vs. period for monochromatic seas and vs. energy period for PM seas.

Conclusions

1. Automated optimisation techniques can improve performance above the previous level of manual optimisation by as much as 30%.

2. The greatest improvements in performance come in the seas with high energy density and energy period (Te).

3. Mounting stiffness can be as much as six times lower than was previously believed with this effect being most pronounced in longer period seas.

4. Power from the spine joints is now of major significance, and the power ratings of electrical plant in the spine must be adjusted accordingly. The design of joint hydraulics will not be affected.

5. The statistical model of the dependence of duck control coefficients on Te and Hrms which was developed on the basis of this series of experiments may be used generally for interpretative purposes. Its use as a predictive model is presently limited to seas with mid-range values of Te and Hrms, until further data become available, and further complexities are introduced to the model.

Results

The results of all the experiments are summarised in Tables 1(a) and 1(b). A complete explanation of how to read these tables is given in Appendix B. Although in three instances the computers did slightly worse than a human operator the average improvement on the manually optimised coefficients was about 10%. Taking account of the individual sea weightings and potential extraction capability of the reference design [9], the average improvement in productivity was 8.7%. This figure was obtained by dividing the sum of the products of "WEIGHT", "Pltd" and "CHANGE" by the sum of the products of "WEIGHT" and "Pltd".

INITIAL / FINAL

SEA DATA				FULL SCALE					TANK SCALE (1/44)				COEFFICIENTS								TEST NUMBER	POWERS				MISC 1					Hrms REAR	Hrms FRONT	OFFSETS			MISC 2	
SEA #	SEA NAME MARTIN EQUIV.	WEIGHT %	RATING	T_e s	H_{rms} m	P_{SEA} kW/m	P_{LTD} kW/m	NOV '81 η %	T_e s	D. CORR H_{rms} cm	P_{SEA} mW		$\dot\theta$ DDC Nm/rad/sec	θ DSC N/rad	$\dot H$ HDC N/m/sec	H HSC N/m	$\dot S$ SDC N/m/sec	S SSC N/m	$\theta\times\dot\theta$ VDC Nm/rad/sec			HEAVE mW	SURGE mW	NOD mW	TOTAL mW	η %	CHANGE %	# RUNS	TORQUE LIMIT Nm	HUB DEPTH cm	WAVE GAUGE A cm	WAVE GAUGE B cm	NOD TORQUE OFFSET Nm	HEAVE FORCE OFFSET N	SURGE FORCE OFFSET N	DATE /83	COMMENTS
359	SEA41:3.11 120R107	3·04	1	12·53	1·09	117·00	59·44	50·8	1·059	0·814	156·76		0·075	0·000	3·000	500·000	30·000	200·000	0·005		01B	5·5	27·7	43·2	76·4	48·7	10·3	247	0·056	6·3	0·598	0·866	-0·005	-0·29	-0·04	30/3	1 capsize initially. None finally.
													0·075	-0·176	11·112	128·600	41·376	140·600	0·005			18·6	32·8	32·9	84·3	53·8					0·603	0·868	-0·006	-0·02	-0·03		
244	SEA15:4.21 80R72	4·14	2	8·98	0·75	40·21	30·00	74·6	0·759	0·543	53·19		0·060	0·000	10·000	200·000	20·000	600·000	0·005		02B	4·0	6·6	27·4	38·0	71·4	4·5	152	0·056	6·3	0·212	0·571	-0·003	0·15	-0·04	3/4	
													0·060	-0·049	13·984	559·600	31·136	511·200	0·005			5·6	8·7	25·4	39·7	74·6					0·224	0·578	-0·003	0·23	-0·03		
388	SEA35:5.71 120R160	1·85	3	11·71	1·73	275·83	63·02	22·8	0·990	1·283	369·04		0·075	-0·100	3·000	500·000	30·000	200·000	0·005		03	15·1	43·7	58·9	117·7	32·0	14·2	144	0·056	6·3	1·031	1·384	-0·005	-0·60	0·06	4/4	4 capsizes initially and finally.
													0·085	-0·031	3·000	213·200	41·328	202·400	0·005			27·0	48·4	59·0	134·4	36·4					1·035	1·373	-0·007	-0·39	-0·00		
171	SEA17:5.24 100R55	5·24	4	9·07	0·58	24·29	18·03	74·2	0·767	0·419	32·13		0·060	-0·100	3·000	700·000	30·000	800·000	0·005		04	1·9	7·6	16·2	25·7	80·0	2·3	246	0·056	6·3	0·203	0·450	-0·003	-0·01	0·04	5/4	
													0·069	-0·100	2·232	868·000	30·816	642·800	0·008			2·5	7·1	16·7	26·3	81·9					0·197	0·458	-0·003	-0·15	0·00		
292	SEA27:3.78 100R90	1·93	5	10·31	0·92	68·84	46·14	67·0	0·871	0·673	91·89		0·060	-0·050	3·000	700·000	30·000	500·000	0·005		05	4·5	17·9	41·2	63·6	69·2	4·6	196	0·056	6·3	0·392	0·720	-0·005	-0·04	-0·02	6/4	
													0·058	-0·033	8·040	550·000	39·992	500·000	0·000			10·3	20·5	35·7	66·5	72·4					0·402	0·712	-0·006	-0·01	-0·02		
371	SEA45:4.00 130R142	1·38	6	12·67	1·45	208·33	63·02	30·3	1·071	1·085	280·51		0·085	0·000	10·000	700·000	30·000	950·000	0·005		06	10·4	46·9	52·2	109·5	39·0	21·2	303	0·056	6·3	0·843	1·179	-0·005	-0·43	-0·12	7/4	
													0·075	-0·175	4·864	112·000	32·736	52·800	0·006			30·1	56·9	45·7	132·7	47·3					0·853	1·183	-0·007	-0·08	-0·10		
377	SEA16:6.89 100R125	1·38	7	9·05	1·21	103·79	61·83	59·6	0·765	0·875	139·52		0·060	0·000	3·000	700·000	30·000	300·000	0·005		07	7·7	26·6	46·1	80·4	57·6	13·8	831	0·056	6·3	0·546	0·993	-0·003	0·17	-0·01	8/4	
													0·067	-0·063	6·984	343·600	28·656	302·400	0·006			18·3	27·8	45·4	91·5	65·6					0·553	1·021	-0·004	-0·02	-0·06		
201	SEA10:3.14 80R55	5·80	8	8·72	0·53	19·46	14·48	74·4	0·737	0·382	25·79		0·060	0·000	10·000	700·000	30·000	600·000	0·006		08	1·8	3·9	15·5	21·2	82·2	-0·6	420	0·056	6·3	·156	·405	-0·003	-0·07	0·10	16/4	
													0·081	-0·161	1·360	655·00	37·78	301·00	-0·005			1·3	6·6	13·2	21·07	81·7					·184	·404	-0·003	-0·10	0·10		
359	SEA41:3.11 120R107	3·04	1	12·53	1·09	117·00	59·44	50·8	1·059	0·814	156·76		0·075	0·000	3·000	500·00	30·00	200·0	0·005		01A	4·8	31·5	38·3	74·6	47·6	9·7	495	0·056	6·3	0·593	0·866	-0·005	-0·31	-0·01	25/3	Trygvasin
													0·073	-0·155	10·07	155·2	35·78	170·4	0·005			14·4	35·0	32·4	81·8	52·2					0·591	0·867	±0·006	0·08	0·01		
210	SEA08:5.03 80R55	5·52	9	8·64	0·5	16·99	12·77	75·2	0·73	0·36	22·74		0·060	0·000	10·000	700·0	20·00	600·0	0·005		09	1·7	3·2	13·4	18·5	81·4	1·6	80 (Hydr.)	0·056	6·3	·144	·379	-·003	0·22	0·07	20/4 (83)	
													0·10	0·00	9·23	700·0	36·0	600	-·07			1·6	4·5	12·5	18·8	82·7					·145	·379	-·004	0·05	0·11		
391	SEA32:6.21 120R160	1·10	10	11·22	1·70	259·02	63·02	24·8	0·948	1·252	391·44		0·06	-0·10	3·000	5000	30·00	200·0	0·005		10	9·9	58·6	61·6	130	38·1	20·2	269	0·056	6·3	·969	1·304	0	-0·67	0·07	21/4	7 CAPSIZES!
													0·09	-0·07	4·392	161·6	33·46	88·4	0·004			29·6	73·5	53·0	156·2	45·7					·982	1·315	-0·001	-0·24	0·05		
322	SEA40:3.27 120R107	1·10	11	12·37	1·11	119·01	61·69	51·8	1·045	0·828	160·49		0·075	-0·10	3·000	500·0	30·00	200·0	0·005		11	6·5	30·7	47·8	85·0	53·0	4·2	856	0·056	6·3	·58	0·859	-0·004	-0·05	0·04	22/4	WEEKEND RUN
													0·086	-0·173	12·5	226·4	28·6	170·0	0·005			16·4	33·8	38·4	88·6	55·2					·593	0·865	-0·005	0·06	0·00		
346	SEA34:3.64 120R107	1·10	12	11·66	1·08	106·15	61·05	57·5	0·985	0·800	143·21		0·075	-0·10	3·000	500·0	30·00	200·0	0·005		12	6·6	26·7	50·0	83·3	58·2	6·3	242	0·056	6·3	·572	·874	-0·005	-0·34	0·04	25/4	
													0·075	-0·176	5·30	195·2	29·46	201·2	0·010			18·2	30·9	39·4	88·6	61·9					·549	·872	-0·007	-0·18	0·03		
291	SEA46:2.41 130R107	1·38	13	13·64	0·99	104·68	46·95	44·9	1·153	0·746	140·77		0·085	-0·10	10·00	700·0	50·00	150·0	0·005		13	3·5	25·0	41·8	70·6	59·2	4·2	298	0·056	6·3	·574	·772	-·006	-0·05	-0·04	27/4	
													0·089	-0·13	7·82	263·2	30·00	121·2	0·001			11·0	28·6	34·1	73·6	52·3											
319	SEA04:5.42 80R72	2·21	14	7·93	0·78	37·85	28·79	76·1	0·670	0·560	50·80		0·06	0·00	10·00	700·0	20·00	600·0	0·005		14A	4·7	7·2	28·1	40	78·7	0	214	0·056	6·3	·222	·638	·003	-·007	0·02	21/4	PROG HUNG-STRIVE- NO POST MORTEM
													0·068	0·039	10·00	700·0	27·14	511·3	0·01			4·4	9·4	26·1	40	78·7					·228	·635	·003	-·002	-0·01		
336	SEA42:3.80 130R125	0·83	15	12·58	1·30	166·90	63·02	37·8	1·063	0·971	223·87		0·085	0·0	10·00	700·0	30·00	150·0	0·005		15	5·1	38·0	54·2	97·3	43·5	12	318	0·056	6·3	·728	1·050	-·005	-0·2	-0·09	28/4	
													0·090	-0·096	8·73	1288	43·4	127·7	0·003			20·9	46·6	41·5	109·1	48·7					·733	1·037	-·006	-0·07	-0·06		
244	SEA15:4.21 80R72	4·14	2	8·98	0·75	40·21	30·00	74·6	0·759	0·543	53·19		0·06	0·00	10·00	700·0	20·00	600·0	0·005		02A	3·5	7·6	29·0	40·1	75·4	2·5	166	0·056	6·3	0·227	0·603	-0·005	-0·01	0·00	28/5	SEE TEST 4
													0·089	-0·113	8·72	700·0	29·22	600·0	0·003			3·3	8·4	29·4	41·1	77·3					0·226	0·598	0·006	-0·01	0·03		
319	SEA04:5.42 80R72	2·21	14	7·93	0·78	37·85	28·79	76·1	0·67	0·56	50·8		0·06	00·00	10·00	700·0	30·00	150·0	0·005		14B	4·6	12·4	22·1	39·1	77·0	6·1	338	0·056	6·3	0·267	0·640	-0·003	0·05	-0·02	28/4	SEE TEST 17
													0·091	0·051	12·2	700·0	63·4	415·6	0·006			4·2	10·8	26·5	41·5	81·7					0·292	0·634	-0·003	-0·07	0·04		
360	SEA38:4.40 100R107	0·83	16	11·85	1·38	177·15	63·02	35·6	1·002	1·025	237·65		0·06	0·0	3·0	7000	30·0	300·0	0·005		16	6·0	31·8	60·6	98·4	41·4	25	348	0·056	6·3	0·732	1·066	-0·003	-0·89	0·06	29/4	
													0·095	-0·069	8·04	64·0	47·0	1584	0·005			26·3	50·3	45·8	122·5	51·6					0·760	1·060	-0·005	-0·35	0·0		
366	SEA16:5.27 80R72	0·83	17	10·50	1·26	129·09	63·02	48·8	0·871	0·921	172·2		0·06	0·0	10·0	700	20·0	600·0	·005		17	7·4	18·9	59·7	85·9	49·9	26	311	0·056	6·3	0·55	1·08	-0·004	-0·88	0·02	1/5	
													0·078	-0·11	10·0	212	33·8	1224	·003			25·5	37·9	46·7	108·3	62·9					0·60	0·974	-0·005	-0·26	0·03		
238	SEA28:2.80 80R55	1·66	18	10·65	0·70	41·66	27·72	66·5	0·90	0·513	54·95		0·06	0·0	10·0	700	20·0	600·0	·005		18	3·1	6·2	28·4	37·6	68·4	11	301	0·056	6·3	0·273	0·575	-0·004	-0·08	0·06	2/5	
													0·068	-0·193	-3·152	467·2	17·6	292·8	0·003			4·1	10·3	27·0	41·8	76·1					0·313	0·577	0·003	0·04	0·04		
220	SEA36:2.78 100R55	1·1	19	11·72	0·83	63·8	38·54	60·4	0·991	0·616	85·02		0·06	-0·10	3·0	7000	30·0	3000	0·005		19	1·9	15·1	36·6	62·5	61·8	8·3	393	0·056	6·3	0·407	0·687	+0·005	0·09	-0·09	29/4	
													0·087	-0·147	6·88	289·6	27·12	207·6	0·003			9·3	19·6	28·0	56·9	66·9					0·429	0·692	-0·005	0·0	-0·04		
324	SEA31:3.65 100R72	0·83	20	11·02	0·97	81·53	50·80	62·3	0·931	0·714	109·2		0·06	-0·05	3·0	7000	30·0	3000	0·005		20	4·0	22·3	42·5	68·8	63·0	3·9	332	0·056	6·3	0·428	0·757	-0·005	-0·28	0·04	29/4	
													0·083	-0·15	4·7	308	30	206	·004			10·8	21·7	39·8	71·5	65·5					0·436	0·742	-0·005	-0·14	0·06		
154	SEA30:2.22 80R37	2·21	21	10·88	0·57	27·50	18·54	67·4	0·920	0·419	37·22		0·06	0·0	10·0	700·0	20·0	600·0	·005		21	2·1	4·1	20·0	26·2	70·4	12·2	331	0·056	6·3	0·22	0·459	(-0·003)	-0·09	0·06	29/4	
													0·073	-0·17	1·168	659·6	18·66	342·4	0·005			2·6	6·5	20·5	29·4	79·0					0·234	0·453	-0·004	0·22	-0·01		
318	SEA05:4.80 60R55	1·66	22	7·95	0·71	31·30	23·81	76·1	0·692	0·510	42·20		0·07	0·0	10·0	1000	30·0	600·0	·005		22	2·3	6·6	23·4	32·0	75·8	2·8	674	0·056	6·3	0·189	0·570	-0·003	0·34	0·07	6/5	
													0·075	-·115	10·0	700·0	34·75	446·4	-·001			3·9	8·2	20·9	32·9	78·0					0·201	0·558	-0·003	0·34	0·08		
218	SEA14:3.24 60R37	2·48	23	8·81	0·55	20·96	15·75	75·1	0·745	0·397	28·06		0·07	0·0	10·0	1000	30·0	600·0	·005		23	1·4	4·7	15·9	22·0	78·4	7·7	327	0·056	6·3	0·147	0·428	-0·003	0·27	0·06	7/5	
													0·053	-·240	2·56	626·8	21·9	344·4	0·005			3·2	8·7	14·9	25·7	84·5					0·188	0·426	-0·003	0·76	0·08		
200	SEA19:2.75 60R37	2·48	24	9·29	0·51	19·30	14·24	73·8	0·785	0·369	25·44		0·07	0·0	10·0	1000	30·0	600·0	·005		24	1·4	4·4	15·9	21·8	85·7	-1·4	282	0·056	6·3	0·158	0·419	-0·002	0·166	0·05	13/5	
													0·085	-0·007	10·0	1000	35·08	600	0·007			1·3	4·8	15·4	21·5	84·5					0·157	0·415	-0·003	-0·03	0·10		
378	SEA22:6.65 60R55	0·55	25	9·52	1·30	126·24	63·02	49·9	0·805	0·943	169·4		0·07	0·0	10·0	1000	30·0	600·0	·005		25	6·7	19·0	67·5	94·6	55·8	11·7	333	0·056	6·3	0·556	1·037	-0·004	-0·6	-0·02	13/5	
													0·093	0·0	20·08	412·0	62·4	336·0	0·006			16·4	32·6	56·8	105·7	62·4					0·552	1·030	-0·003	-0·54	0·04		
381	SEA44:4.14 100R125	0·55	26	13·26	1·62	273·7	63·02	23·0	1·121	1·215	366·4		0·075	0·0	3·0	500·0	30·0	300·0	0·005		26	7·7	42·3	66·1	115·1	31·4	30·8	317	0·056	6·3	0·968	1·399	-0·005	-0·78	0·01	13/5	
													0·080	-0·11	4·39	74·0	37·4	2·4	·007			34·5	68·4	47·7	160·6	41·1					1·002	1·300	0·006	-0·15	0·02		
294	SEA23:4.30 60R55	0·83	27	9·54	0·86	55·14	40·84	74·1	0·806	0·624	74·30		0·07	0·0	10·0	1000	30·0	600·0	·005		27	3·4	9·3	39·8	52·5	70·7	6·3	267	0·056	6·3	0·276	0·708	0·004	-0·06	0·09	17/5	
													0·074	-0·14	2·9	517·6	27·1	360	·010			7·1	13·8	34·8	55·8	75·1					0·327	0·698	0·004	-0·06	0·12		
168	SEA18:3.14 60R37	1·93	28	9·11	0·57	23·53	17·48	74·3	0·770	0·413	31·17		0·07	0·0	10·0	1000	30·0	600·0	·005		28	1·6	4·9	18·5	25·1	80·5	4·8	701	0·056	6·3	0·162	0·444	0·003	0·04	0·12	1/6	
													0·055	-0·19	6·3	1020	6·45	600	0·006			2·5	1·8	22·0	26·3	84·4					0·165	0·441	0·003	0·10	0·12		

Table I(a): Results of optimisation.

INITIAL / FINAL

SEA DATA				FULL SCALE					TANK SCALE (1/149)			COEFFICIENTS							TEST NO.	POWERS				MISC 1				Hrms REAR	Hrms FRONT	OFFSETS			MISC 2	
SEA #	SEA NAME / MARTIN EQUIV	WEIGHT	RATING	T_e	H_{rms}	P_{SEA}	P_{LTO}	NOV '81 η	T_e	H_{rms}	P_{SEA}	$\dot{\theta}$ DDC	θ DSC	$\dot{H}$ HDC	H HSC	$\dot{S}$ SDC	S SSC	$\theta\times\dot{\theta}$ VDC		HEAVE	SURGE	NOD	TOTAL	η	CHANGE	# RUNS	TORQUE LIMIT	HUB DEPTH	WAVE GAUGE A	WAVE GAUGE B	NOD TORQUE OFFSET	HEAVE FORCE OFFSET	SURGE FORCE OFFSET	DATE	COMMENTS
		%		s	m	kW/m	kW/m	%	s	cm	mW	Nm/rad/sec	N/rad	N/m/sec	N/m	N/m/sec	N/m	N/m/rad/sec		mW	mW	mW	mW	%	%		Nm	cm	cm	cm	Nm	N	N	/83	
290	SEA01 : 7·72	1·93	29	6·35	0·68	23·21	17·48	75·3	0·537	0·486	30·92	0·07	0·0	10·0	1080	30·0	600	0·005	29	2·7	6·3	15·9	24·8	80·2	1·6	242	0·056	6·3	·174	·563	-0·003	0·14	0·02	19/5	
352	SEA 33 : 3·42	0·55	30	11·45	0·98	95·13	51·80	60·4	0·968	0·723	115·79	0·086	0·07	20·5	1080	37·2	574	0·006		2·9	6·8	15·6	25·2	81·5					·147	·559	-0·003	0·12	0·02		
242	SEA 46 : 1·59	1·1	31	14·58	0·71	58·24	25·13	43·1	1·232	0·537	77·39	0·092	-0·174	9·72	368	32·9	328	0·007	30	5·6	27·5	40·3	73·5	63·5	5·7	387	0·056	6·3	·479	·770	-0·005	0·22	0·06	19/5	
223	SEA 39 : 1·88	1·38	32	12·19	0·59	32·98	19·79	60·0	1·030	0·439	44·68	0·069	-0·4	-0·42	114	13·9	70·8	0·007	31	12·0	23·0	42·7	77·7	67·1	17	337	0·056	6·3	·465	·773	-0·005	0·18	0·04		
355	SEA 12 : 5·77	0·55	33	8·76	0·98	66·52	47·97	72·0	0·740	0·707	88·51	0·056	-0·215	0·31	305·6	24·5	270·8	0·004	32	11·6	13·7	21·2	36·5	47·2					·426	·589	-0·007	0·10	0·08		
177	SEA 13 : 3·19	1·66	34	8·78	0·55	21·02	15·70	74·7	0·742	0·317	27·91	0·061	0·0	10·0	700	20·0	600	0·005	33	11·5	15·5	15·6	42·7	55·2	7·7	345	0·056	6·3	·429	·593	-0·005	0·14	0·11	19/5	
249	SEA 20 : 3·80	0·83	35	9·37	0·74	40·56	30·46	75·1	0·792	0·536	54·03	0·067	-0·237	3·0	442·6	30·0	411	0·008	34	2·9	10·5	17·9	31·3	70·1					·290	·868	-0·003	0·11	0·14	23/5	
228	SEA 21 : 3·62	0·83	36	9·51	0·72	39·24	29·11	74·2	0·804	0·522	51·91	0·083	-0·11	9·43	719·2	30·3	435·6	0·005		5·6	9·1	19·0	33·7	75·4	7·7	345	0·056	6·3	·295	·474	-0·005	0·17	0·13		
347	SEA 11 : 5·44	0·55	37	8·75	0·92	57·74	43·74	75·8	0·74	0·664	77·99	0·093	-0·10	14·5	389·2	48·2	310·8	0·005	35	7·3	10·9	45·3	63·5	71·7					·346	·801	-0·004	0·06	0·01	24/5	
267	SEA 25 : 2·78	1·1	38	10·0	0·62	30·23	21·64	71·6	0·845	0·452	40·48	0·07	-0·1	6·02	700	35·8	399·8	0·007		10·3	18·3	38·9	67·5	76·2	6·3	335	0·056	6·3	·355	·794	-0·004	0·08	0·07		
180	SEA 06 : 3·32	1·66	39	8·39	0·52	17·76	13·43	75·5	0·709	0·374	23·87	0·062	-0·214	1·43	700·0	20·0	435·6	0·005	36	2·3	3·8	18·2	24·2	86·5					·164	·437	·003	·007	0·05	24/5	Thruster needs rebuilding
241	SEA 29 : 2·19	1·1	40	10·83	0·54	25·13	16·65	66·3	0·915	0·397	33·25	0·083	-0·276	-3·19	575	11·2	300	0·005		2·3	3·8	18·2	24·2	86·5	0·0	67	0·056	6·3	·164	·439	-0·003	0·07	0·05		
108	SEA 09 : 2·92	1·1	41	8·71	0·47	15·23	11·37	74·7	0·736	0·339	19·73	0·086	0·23	7·5	1025	20·0	600·0	0·005		2·6	11·8	26·3	40·7	75·3	5·4	260	0·056	6·3	·271	·593	-0·003	0·08	0·06	24/5	
268	SEA 02 : 5·05	0·55	42	7·60	0·67	30·23	21·64	71·6	0·642	0·480	35·92	0·084	-0·061	10·0	5360	26·4	600	0·003	37	6·4	9·9	26·7	42·9	79·4					·278	·590	-0·004	0·03	0·06		
89	SEA 24 : 1·93	1·1	43	9·95	0·42	13·87	9·92	71·5	0·841	0·365	18·48	0·073	-0·1	3·0	700	30	302	0·005		2·6	11·0	26·1	39·8	76·7	3·5	364	0·056	6·3	·267	·586	-0·003	0·003	0·04	25/5	
112	SEA 37 : 1·69	0·83	44	11·72	0·46	19·2	12·28	64·0	0·991	0·342	25·75	0·04	-0·20	-7·6	399·2	14·16	342·8	0·006		3·7	9·2	28·4	41·2	79·4					·248	·587	-0·004	0·04	0·05		
212	SEA03 : 3·36	0·83	45	7·87	0·47	13·83	10·32	74·6	0·665	0·337	18·31	0·06	0·0	-0·46	509·6	44·4	422·4	0·005	38	4·4	16·6	37·0	58·1	74·5	5·9	341	0·056	6·3	·368	·727	-0·003	-0·65	0·12	23/5	
122	SEA01 : 2·42	1·1	46	8·62	0·38	9·98	7·31	74·5	0·729	0·279	13·11	0·06	0·0	10·0	700	20·0	600	0·005		11·0	17·5	33·0	61·5	78·9					·342	·729	-0·003	-0·04	0·13		
												0·073	0·0	4·29	700	26·8	434·4	0·005		2·0	8·2	19·7	29·8	73·6	0·3	361	0·056	6·3	·225	·512	-0·003	-0·05	0·00	23/5	
																				2·1	8·2	19·7	29·9	73·9					·219	·510	-0·003	-0·05	0·07		
																			39	1·7	3·5	14·5	19·7	82·5	6·6	347	0·056	6·3	·141	·445	±0·003	·005	-0·01	29/5	
																				2·1	4·1	14·9	21·0	87·9					·158	·440	-0·002	0·16	0·01		
																			40	1·6	6·2	15·1	22·9	68·9	3·5	290	0·056	6·3	·208	·425	-0·003	0·09	0·02	29/6	
																				2·2	4·8	16·6	23·7	71·3					·223	·433	-0·003	0·24	0·04		
																			41	1·4	2·4	11·7	15·6	79·1	3·2	88	0·056	6·3	·137	·361	-0·003	-0·04	0·10	30/5	
																				1·0	2·5	12·6	16·1	81·6					·130	·362	-0·003	-0·05	0·09		
																			42	3·2	5·2	19·3	27·7	77·1	2·2	242	0·056	6·3	·187	·555	-0·003	0·03	0·03	30/6	
																				3·1	6·3	18·9	28·3	78·8					·185	·554	-0·003	-0·05	0·06		
																			43	1·1	3·1	8·0	12·5	66·6	-4·9	91	0·056	6·3	·134	·309	-0·003	-0·03	0·05	31/5	
																				1·0	3·2	7·5	11·7	63·3					·130	·300	-0·003	-0·10	0·05		
																			44	2·1	6·2	11·2	19·5	75·7	7·2	249	0·056	6·3	·213	·356	-0·003	0·02	0·06	21/5	
																				0·9	3·8	16·3	20·9	81·2					·224	·359	-0·003	-0·11	0·03		
																			45	1·7	2·8	9·1	13·5	73·7	8·1	336	0·056	6·3	·137	·582	-0·003	0·03	-0·01	1/6	
																				1·5	4·9	8·7	14·6	79·7					·153	·577	-0·003	-0·02	0·07		
																			46	1·1	2·0	7·9	11·0	83·9	3·6	376	0·056	6·3	·104	·246	-0·003	0·11	0·07	1/6	
																				1·1	3·3	7·0	11·4	87·0					·116	·296	-0·003	0·06	0·03		

Table I(b): Results of optimisation.

Figure 4 shows a typical time history for the optimisation of one sea. Percentage increase in output power is plotted against run number. As the optimisation proceeded, it steadily became more and more difficult to make an improvement. The data for this curve should be fitted fairly well by a function of the type:-

$$\% \text{ Increase} = \text{Max Increase} \left[1 - \exp(-\alpha t)\right]$$

where α is a constant and t is the run number.

During the course of the experiments it was noted that the system would produce the same optimised coefficients when started with different initial coefficients in a particular sea. It was also observed that in some cases, for example sea #359, the control system was able to learn to avoid capsizing.

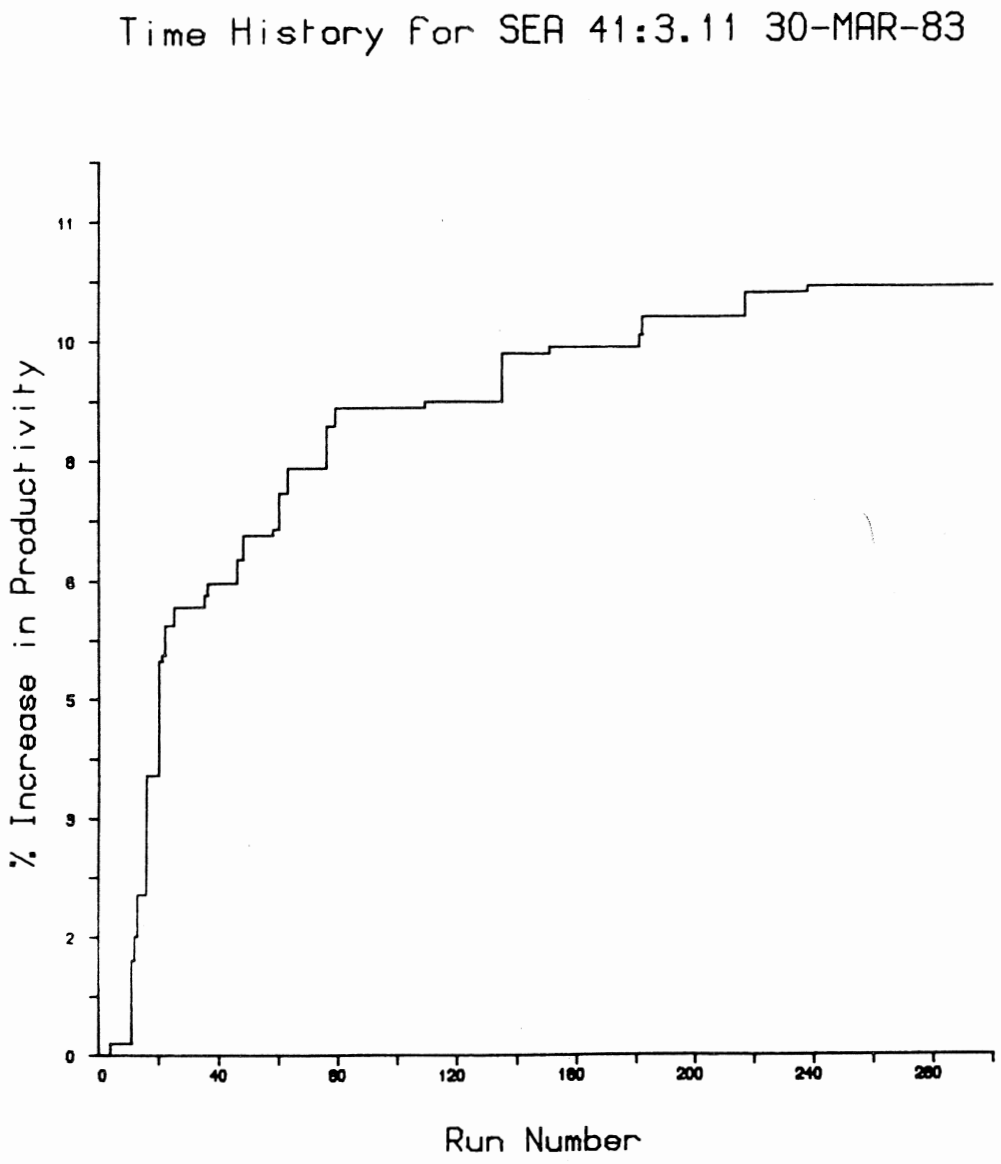

Figure 4: Improvement time history for a typical optimisation.

Figures 5(a) and 5(b) show the percentage increase in total power plotted against the full-scale sea power and energy period respectively for each of the 46 seas. As might be expected, the largest improvements were made in the more energetic seas, and also tended to be made in those with large Te values. It is useful to note that,

$$P_{SEA} = \frac{\rho g^2}{4\pi} H_{rms}^2 T_e \qquad \frac{\rho g^2}{4\pi} = 7.82 \text{ kW m}^{-1}$$

where ρ is the water density and g is the local acceleration due to gravity.

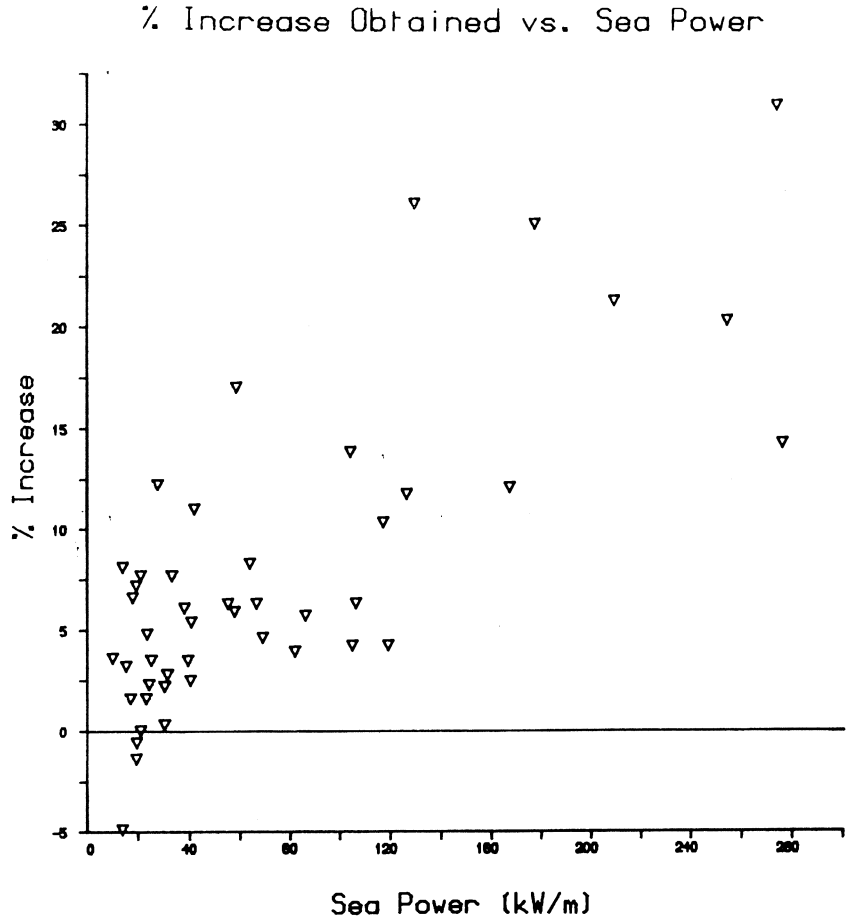

(a)

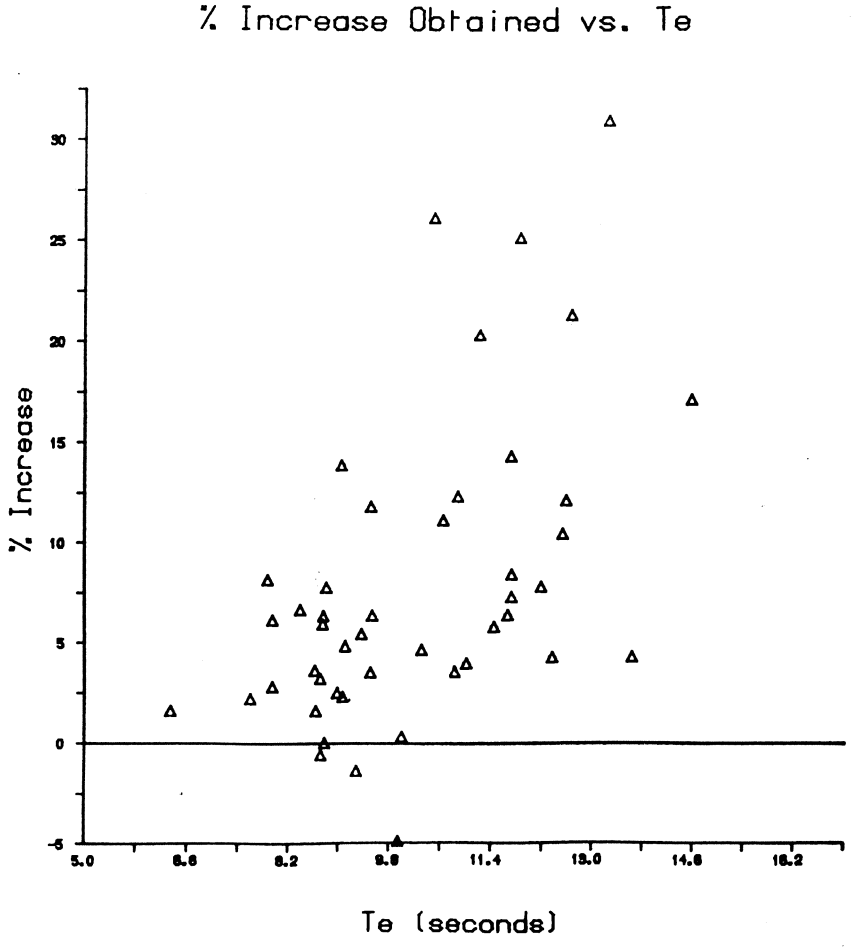

(b)

Figure 5: Percentage increase in total power vs. (a) full scale sea power and (b) full scale energy period.

Figure 6 shows a "bubble plot" of optimised duck efficiency against energy period for the 46 spectra. The Te axis has been weighted according to the power available at any particular Te value in the No. 1 series of measurements off South Uist. The radius of each bubble is proportional to the power extracted by the duck and its mounting with no power limit. This plot shows the expected trend that the duck is more efficient in low Te and low power seas. The results of the optimisation are summarised in a form useful for a productivity analysis in Table II, which shows each of the 46 spectra with its IOS spectrum number, and full-scale total power output.

IOS Spectrum	KW Full Scale
89	400
108	570
112	710
122	390
154	990
168	900
171	910
177	830
180	710
200	740
201	720
210	640
212	500
218	810
220	1940
223	1130
228	1420
238	1440
241	820
242	1460
244	1410
249	1470
267	1020
268	1080
280	860
291	2490
292	2270
294	1880
318	1110
319	1410
322	2990
324	2430
336	3700
346	2990
347	2070
352	2620
355	2310
359	2860
360	4160
366	3690
371	4480
377	3100
378	3580
381	5120
388	4570
391	5280

DUCK TORQUE LIMIT = 0.056 Nm

MOUNTING FORCE LIMIT = 3.0 N

NO POWER LIMIT

SCALE 140

Table II: Optimised output at full scale.

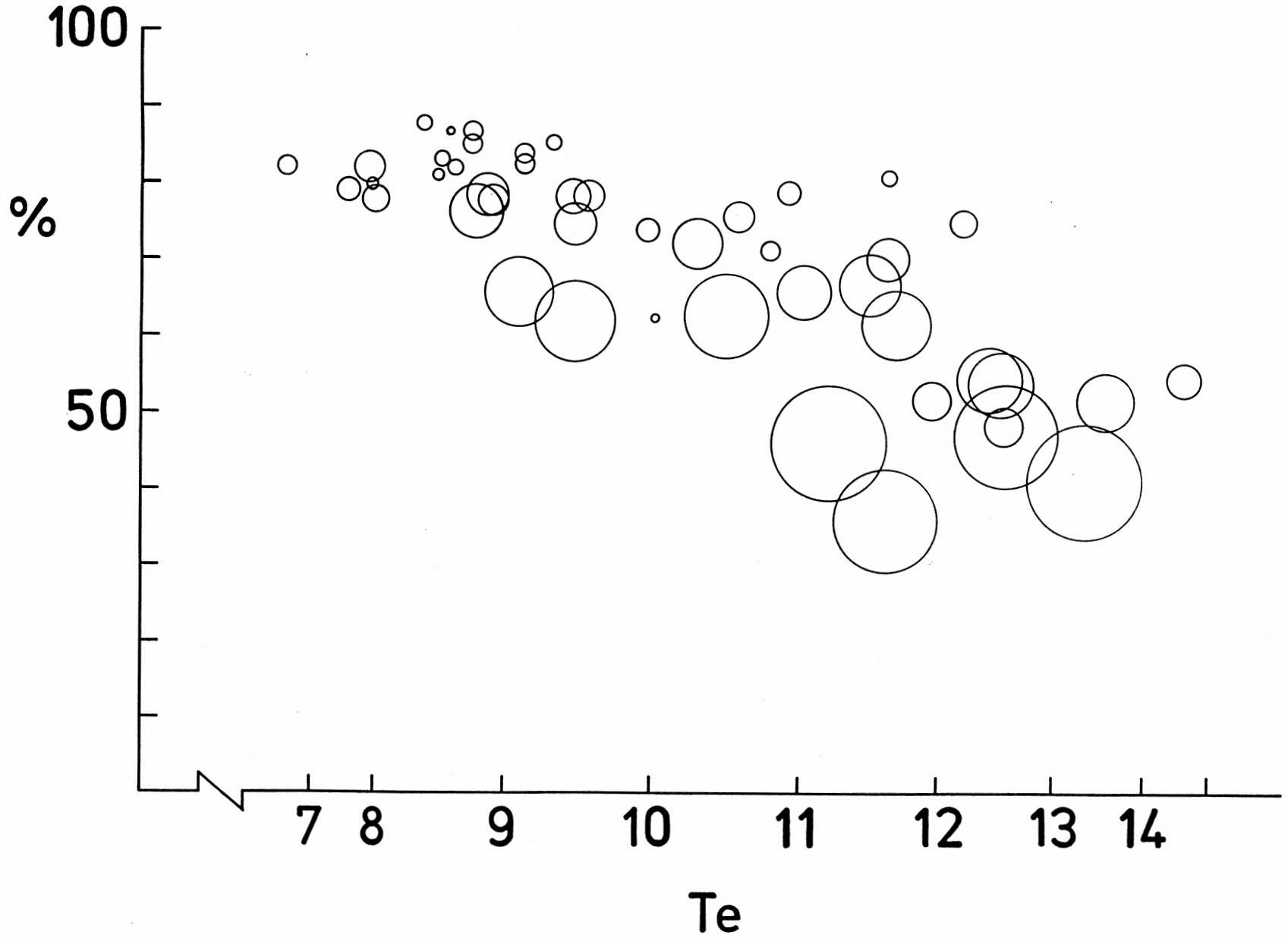

Figure 6: Bubble plot of optimised duck efficiency against energy period with the Te axis weighted with the power available in the no.1 South Uist seas. Efficiency calculations are based on the power across the whole width of the tank. The model occupied 0.76 of this width.

Some interesting points emerge on examination of the power distribution between the modes before and after optimisation. Glancing down the "POWER" columns on Table 1 it can be seen that, in most of the seas, the spine power (heave power and surge power) increased at the expense of nod power, which decreased a little. This is shown in Figure 7(a) and 7(b) where the change in percentage contribution of spine power to total output is plotted against sea power and Te. It indicates a slight bias towards improving the nod power, rather than the total power during the previous manual optimisations. In fact in many of the seas with large Te values more power can be extracted from the spine than from the nod motions. Thus it will be necessary to change the reference design of 1981[10] which only allotted 1/12 of the duck's generating capacity to the spine joints.

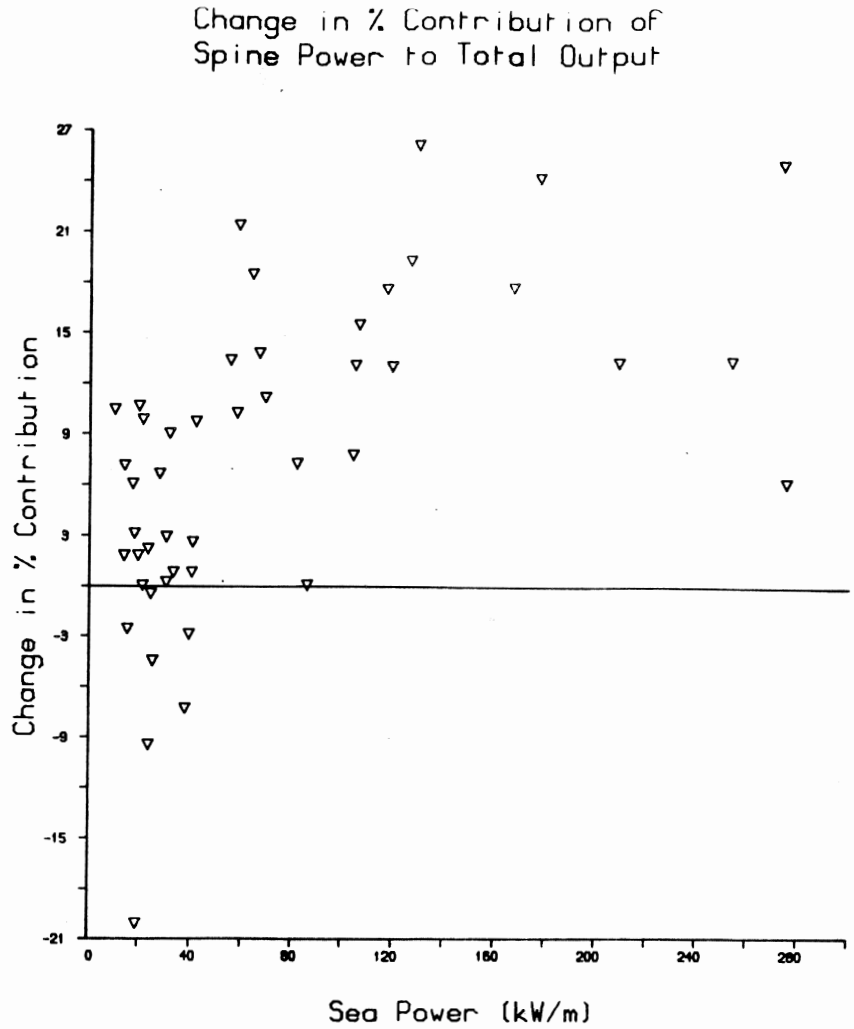

(a)

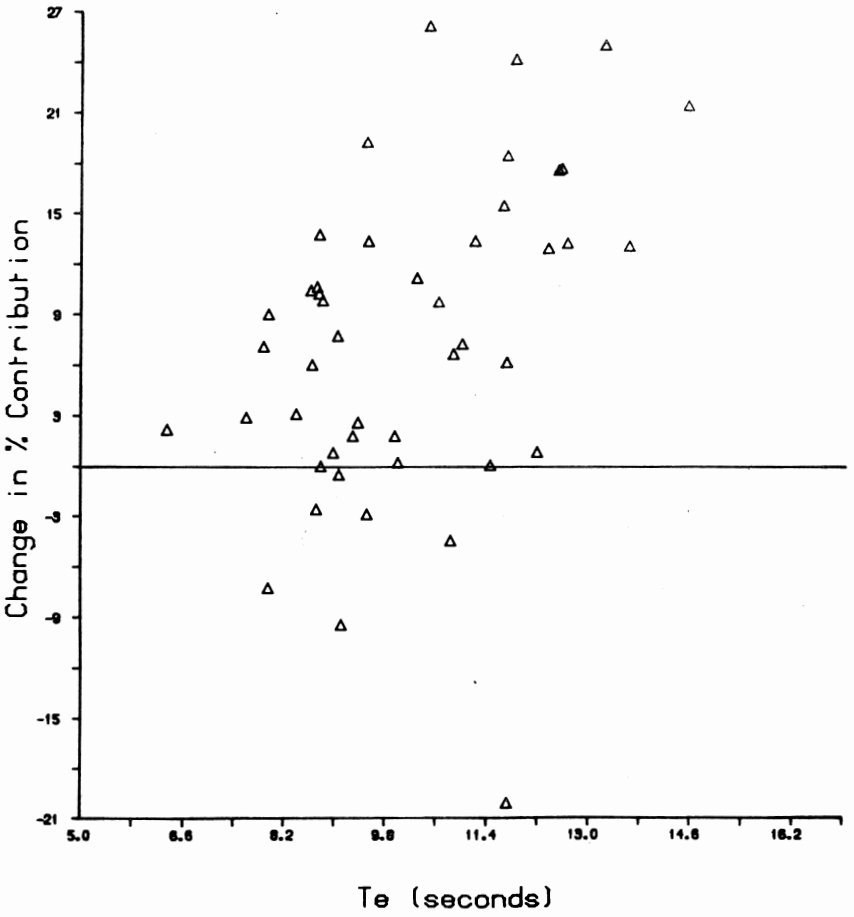

(b)

Figure 7: Percentage change in contribution of spine power to total power vs. (a) full scale sea power and (b) full scale energy period.

Statistical Analysis of the Results

In order to make sense of the results of the optimisations, a lengthy statistical analysis was carried out. The dependence of the seven duck control coefficients on energy period (Te) and wave height (Hrms) was examined, and a statistical model developed. It was found that the two coefficients DDC and VDC ($\dot{\theta}$ and $\theta \times \dot{\theta}$) vary independently of Te and Hrms and that the five remaining coefficients may be modelled with varying degrees of success. Confidence intervals were also developed for the estimated values of the duck control coefficients. In conclusion, it was found that the statistical model provides one with an overall view of the dependence of the coefficients on Te and Hrms, although the variability is too large to enable prediction of individual responses to predetermined values of the two factors.

The first move was to plot the 'responses' against the supposed 'explanatory variables'. Appendix D contains a series of scatter diagrams displaying firstly the individual coefficients against individual factors (Figures D.1 to D.14) and secondly the variation of each coefficient with both factors simultaneously (figures D.15 to D.21). It is immediately apparent that a high degree of variability exists, and that closely fitting models are unlikely to be developed. Thus any use of the fitted equations for predictive, as opposed to interpretive, purposes must be approached cautiously. It is difficult to spot visually any trends, except in the case of Figures D.7, D.8 and D.18, which show a strong dependence of the heave spring coefficient on Te and Hrms, and similarly for the surge spring coefficient in Figures D.11, D.12 and D.19.

After a series of preliminary tests, it was found that:-

(i) $\dot{\theta}$, $\dot{S}$ and $\theta \times \dot{\theta}$ are independent of Te, with θ, $\dot{H}$, H and S all showing significant negative correlation with Te.

(ii) $\dot{\theta}$, θ, H and $\theta \times \dot{\theta}$ are independent of Hrms, while H and S show negative correlation and $\dot{S}$ shows positive correlation with Hrms.

(iii) Te and Hrms are positively correlated, which was already known.

The third of these made it necessary to consider multiple correlation coefficients which give a measure of how a response depends simultaneously on two factors.

As a result of further tests, it was decided to fit a full second order model. It was thought that this would be sufficient since any higher degree terms would complicate the analysis unnecessarily and, in any event, contribute little in the way of improvement to the fit. This model can be expressed as:-

$$Y = b_0 + b_1 X_1 + b_2 X_2 + b_3 X_3 + b_4 X_4 + b_5 X_5 + \varepsilon$$

where **Y** is a particular coefficient to be modelled, b_i $(i = 0 \text{ to } 5)$ are constants, X_i $(i = 1 \text{ to } 5)$ are respectively Te, Hrms, Te^2, $Hrms^2$ and TeHrms, and ε is a normally distributed random variable denoting the random variation about the fitted regression line.

The results of the regression analysis are shown below as seven equations. The 95% confidence interval for each equation can be found in Appendix E. It should be stressed that the confidence interval does not imply that, if we chose Te and Hrms, then the response would be in our interval with 0.95 probability. The variability involved in predicting an individual value is considerably larger and for the given data set makes the intervals ridiculously large in all cases. Only confidence intervals for the means were developed.

$$\theta = 0.0015 - 0.289Te^2 + 0.179TeHrms$$

$$\dot{\theta} = 0.0772$$

$$\theta_* \dot{\theta} = 0.0045$$

$$H = 1.6 + 2656Te - 484Hrms - 1967Te^2$$

$$\dot{H} = 0.056 - 20.56Te + 64.7Hrms - 35.7Hrms^2$$

$$S = 2.8 + 1529Te - 1082Te^2 - 278TeHrms$$

$$\dot{S} = 0.32 + 59.7Te + 27.3Hrms - 49.5Te^2$$

The Te and Hrms values that are used should be at tank scale (1:140) and have units of seconds and centimetres respectively.

Testing the Statistical Model

In order to test the model's predictive, rather than interpretative validity, four sets of seas (25 in total) were selected and the required duck control coefficients were predicted for each one. The four sea sets were as follows:

1. A set of ten seas representing an evenly distributed sample of the "46".

2. A set of five extreme seas.

3. A set of five interior seas close to the set of ten.

4. A set of five interior seas distant from the set of ten.

Figure 8 shows a Te vs Hrms scatter diagram for the four sea sets. It can be seen that the extreme seas are external to the set of ten in the Te Hrms plane, and that the interior seas are within the area covered by the set of ten, with the "interior seas close to the set of ten" being more closely packed.

Each sea was run with first the optimised duck control coefficients, and then the predicted coefficients. The results of these tests are shown in Table III. The figure in the "CHANGE" column is the percentage difference between optimised and model powers. Thus if the value is positive, the predicted coefficients are better than the 'optimised' ones in that particular sea. Figures 9(a) to 9(d) show this value plotted against the full-scale sea power for each of the four sets of seas with Te and Hrms values plotted. In the set of ten seas and the set of five extreme seas (figures 9(a) and 9(b) respectively), the model does not predict better coefficients on the whole, improving the productivity in four out of ten and two out of five seas respectively. However, in both sets of interior seas (Figures 9(c) and 9(d)) the model produces better coefficients in three out of five cases. The general trend shown by the four scatter diagrams is that the model predicts well in very low power seas where the duck is operating in a linear regime. It is not so successful in the larger seas, where non-linear effects, the torque limit and mounting force limits come into play. These non-linearities could be accounted for in a more complex model.

However, in order to compare the predicted and optimised coefficients realistically, some attention must be given to sea powers and weights. This explains the relevance of the additional column in Table III labelled as "Pltd WEIGHT CHANGE PRODUCT" in the bold box. This figure indicates the relative effect that using the model, as opposed to the optimised coefficients, would have on productivity. The sum of the "PWC" numbers for each of the four sets of seas is also given. It can now be seen that, from the point of view of productivity, the model is only successful for the set of five interior and close seas. These seas all have mid-range values of Te and Hrms. It is reasonable to expect that it is in this region that the model works best, rather than at the extremes. However, the model is not generally successful, as is reflected by the Σ PWC figure for the set of ten seas.

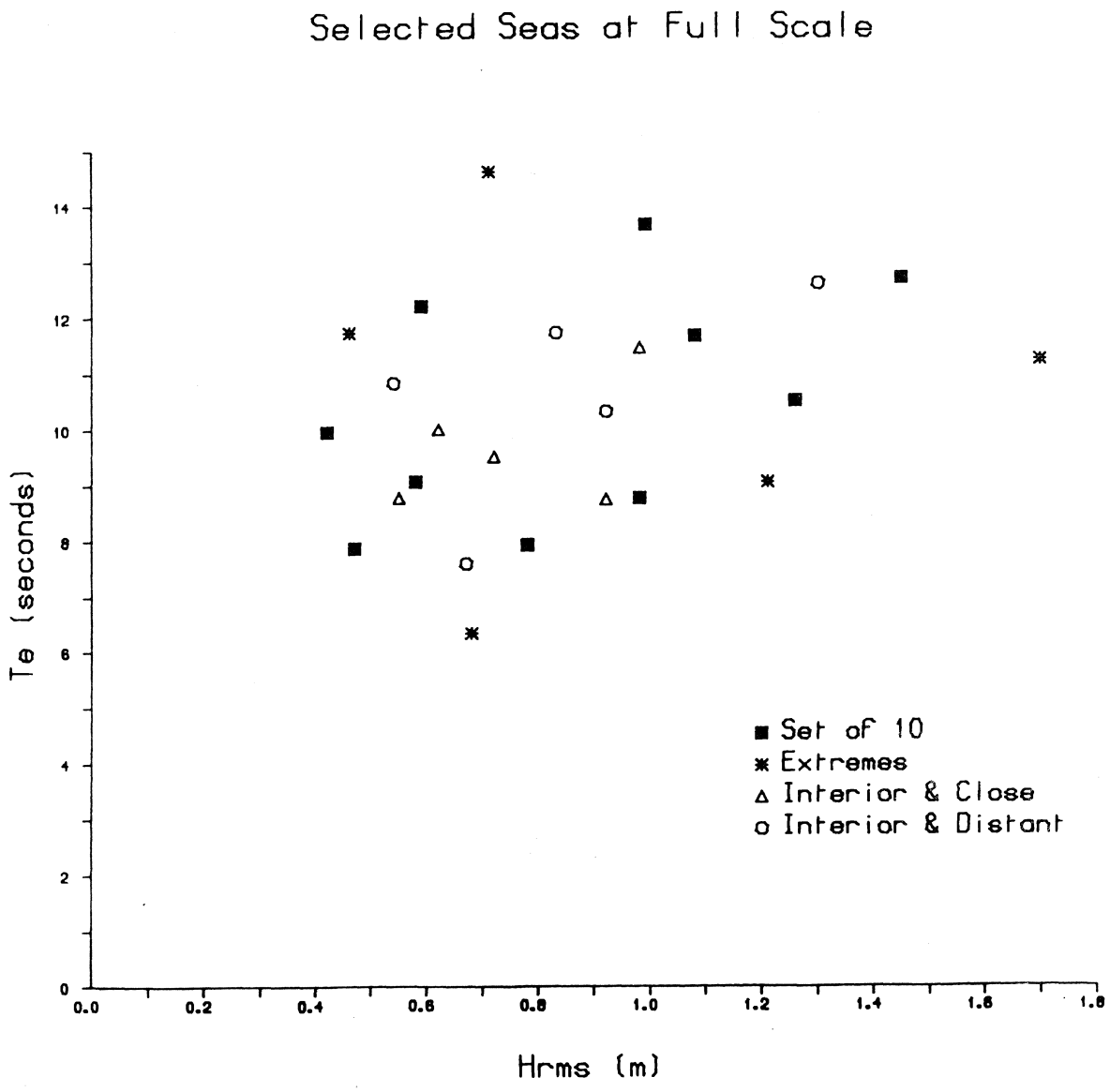

Figure 8: Te vs. Hrms scatter diagram of the four sets of seas chosen to test the statistical model of the duck control coefficients.

OPTIMISED MODEL

SEA #	SEA NAME / MARTIN EQUIV	WEIGHT %	RATING	FULL SCALE T_z s	FULL SCALE H_{rms} m	FULL SCALE P_{SEA} kW/m	FULL SCALE P_{STD} kW/m	FULL SCALE NOV '81 η %	TANK SCALE (1/40) T_z s	TANK SCALE (1/40) Ω corr H_{rms} cm	TANK SCALE (1/40) P_{SEA} mW	COEFFICIENTS $\dot{\theta}$ DDC deg/sec	θ DSC deg/deg	$\dot{H}$ HDC m/sec	H HSC m	$\dot{S}$ SDC m/sec	S SSC m	$\theta\times\dot{\theta}$ VDC deg/sec	Auto WEIGHT CHANGE PROJECT	POWERS HEAVE mW	SURGE mW	NOD mW	TOTAL mW	η %	CHANGE %	# RUNS	TORQUE LIMIT Nm	HUB BMOM cm	H_{rms} REAR WAVE GAUGE A cm	H_{rms} FRONT WAVE GAUGE B cm	OFFSETS NOD TORQUE OFFSET Nm	HEAVE FORCE OFFSET N	SURGE FORCE OFFSET N	DATE /83	COMMENTS
212	SEA05: 3·50	0·83	45	7·87	0·47	13·83	10·32	74·6	0·665	0·337	18·31	0·006	0·0	-0·46	509·6	44·4	422·4	0·005	+57	1·4	4·0	8·0	18·5	73·7	+6·7%		0·056	6·3						18/8	Set of 10
												0·076	-0·086	4·133	734·9	27·33	4798	0·005		1·5	3·5	9·4	14·4	78·6												
171	SEA17: 3·24	5·24	4	9·07	0·58	24·29	18·03	74·2	0·767	0·449	32·13	0·009	-0·100	2·232	568·0	20·816	442·8	0·008	-113	2·9	6·1	17·0	26·0	81·0											18/8	
												0·076	-0·111	0·128	678·8	28·4	449·7	0·005		2·6	6·7	17·5	25·7	80·0	-1·2		0·056	6·3							
089	SEA24: 1·93	1·10	43	9·95	0·42	13·87	9·92	71·5	0·884	0·305	18·46	0·013	-0·100	8·00	700·0	80·0	302·0	0·005	+37	1·1	4·2	9·2	14·5	78·5											18/8	
												0·076	-0·157	-0·822	696·4	25·8	452·1	0·005		0·9	3·2	11·0	15·0	81·2	+3·4		0·056	6·3							
319	SEA04: 5·42	2·21	14	7·93	0·78	35·85	28·79	78·1	0·670	0·680	50·80	0·068	0039	1000	7000	27·48	511·3	0·010	+165	5·0	8·0	85·0	38·0	76·8											18/8	
												0·076	-0·061	11·82	627·1	83·4	437·2	0·005		6·1	9·2	23·7	39·0	76·7	+2·6		0·056	6·3							
355	SEA12: 5·77	0·55	33	8·76	0·98	66·52	47·87	72·0	0·760	0·707	88·59	0·010	-0·129	13·9	508	44·5	374	-0·002	-16	11·5	10·3	34·9	62·6	70·7											18/8	
												0·076	-0·055	12·7	542·7	36·7	396·3	0·005		10·2	15·8	36·3	62·2	70·2	-0·6		0·056	6·3							
366	SEA26: 6·25	0·83	17	10·50	1·26	129·09	63·02	48·8	0·871	0·921	172·2	0·078	-0·110	10·0	818·0	38·8	182·4	0·005	-293	23·7	23·7	42·6	102·1	59·3											18/8	
												0·076	-0·074	11·5	3770	39·9	290·7	0·005		17·5	30·4	48·5	96·4	58·0	-5·6		0·056	6·3							
246	SEA34: 3·64	1·10	12	11·66	1·08	105·15	61·05	57·5	0·965	0·800	144·31	0·075	-0·176	5·30	195·2	29·46	201·2	0·010	-161	18·0	29·8	34·9	82·6	57·7											19/8	
												0·076	-0·138	8·72	322·1	32·94	240·0	0·005		13·9	26·6	40·2	80·6	56·3	-2·4		0·056	6·3							
223	SEA 39: 1·88	1·38	32	12·19	0·59	32·98	19·79	60·0	1·030	0·439	44·68	0·056	-0·215	0·31	305·6	24·5	270·8	0·004	-55	5·0	8·0	17·6	30·7	69·6											19/8	
												0·076	-0·220	0·402	438·0	21·3	304·1	0·005		3·3	7·1	19·7	30·1	67·5	-2·0		0·056	6·3							
571	SEA44: 4·00	1·38	6	12·67	1·45	208·33	63·02	30·3	1·071	1·085	280·51	0·075	-0·175	4·846	116·0	32·736	52·800	0·006	+122	30·7	51·7	40·6	123·0	43·8											19/8	
												0·076	-0·132	6·209	64·8	37·1	76·2	0·004		21·1	54·8	38·7	124·7	44·4	+1·4		0·056	6·3							
291	SEA45: 2·41	1·38	13	13·68	0·99	104·88	46·95	44·9	1·153	0·746	140·77	0·089	-0·13	7·82	2882	80·0	121·2	0·001	-7	10·4	27·2	30·4	67·9	48·3											19/8	
												0·076	-0·229	4·769	87·9	23·7	88·2	0·005		17·1	29·5	21·2	67·8	48·1	-0·1		0·056	6·3							
																			Σpvc	-264															
280	SEA01: 7·72	1·93	29	6·35	0·68	23·21	17·48	75·3	0·537	0·486	30·90	0·086	0·07	20·5	1080	37·2	574	0·006	-121	8·0	6·0	15·6	24·6	79·7											19/8	Extremes
												0·076	-0·038	12·0	625·4	51·4	439·3	0·005		4·2	6·7	12·8	21·7	76·7	-3·6		0·056	6·3							
242	SEA46: 1·59	1·1	31	14·58	0·71	58·24	25·13	43·1	1·232	0·537	77·39	0·069	-0·4	-0·92	114	13·9	70·8	0·007	-116	10·7	13·2	14·1	37·9	49·0											19/8	
												0·076	-0·184	-0·825	29·32	15·4	60·3	0·005		11·1	15·7	9·5	36·3	46·9	-4·2		0·056	6·3							
377	SEA16: 6·89	1·38	7	9·05	1·21	103·79	61·93	59·6	0·765	0·875	139·52	0·067	-0·063	6·994	345·6	28·656	202·4	0·006	+188	21·4	27·7	44·3	90·4	64·8											20/8	
												0·076	-0·098	13·607	458·8	40·91	353·2	0·005		18·7	25·7	47·9	92·4	66·2	+2·2		0·056	6·3							
112	SEA37: 1·68	0·83	44	11·72	0·46	19·2	12·28	64·0	0·991	0·362	25·75	0·070	-0·20	-7·6	399·2	14·76	582·8	0·006	+57	-0·62	3·4	16·8	19·7	76·4											21/8	
												0·076	-0·222	-2·37	536·4	20·20	361·2	0·005		1·7	3·8	15·3	20·8	80·8	+5·6		0·056	6·3							
391	SEA32: 6·21	1·10	10	11·22	1·70	259·08	63·02	24·8	0·948	1·262	34·44	0·09	-0·07	9·392	161·6	33·46	86·4	0·004	-35	31·2	69·9	47·2	148·3	43·4											21/8	
												0·076	-0·05	5·610	145·8	46·6	149·9	0·005		30·1	69·9	47·6	147·6	43·2	-0·5		0·056	6·3							
																			Σpvc	-27															
177	SEA15: 3·19	1·66	34	8·78	0·55	21·02	15·70	74·7	0·742	0·397	27·87	0·061	0·0	10·6	700	80·0	600	0·005	+78	2·3	3·5	17·5	23·2	83·4											22/8	Interim + close
												0·076	-0·105	4·86	617·2	26·2	459·7	0·005		2·4	4·9	16·7	23·9	85·9	+3·0		0·056	6·3							
228	SEA21: 3·42	0·83	36	9·51	0·72	39·24	29·11	74·2	0·804	0·522	51·91	0·083	-0·11	9·43	719·2	30·3	435·6	0·005	+48	3·7	8·2	27·7	39·6	76·2											22/8	
												0·076	-0·11	7·67	612·9	30·6	416·0	0·005		4·5	8·8	27·2	40·4	77·9	+2·0		0·056	6·3							
267	SEA25: 2·78	1·1	38	10·0	0·62	30·23	21·64	71·6	0·845	0·452	40·48	0·070	-0·10	6·02	700	35·8	319·9	0·007	+86	2·3	7·6	20·3	30·2	74·6											22/8	
												0·076	-0·136	4·634	622·7	27·8	416·1	0·005		2·9	6·4	22·0	31·3	77·3	+3·6		0·056	6·3							
352	SEA33: 3·42	0·55	30	11·45	0·98	85·73	51·80	60·4	0·968	0·723	115·79	0·092	-0·174	9·72	368	32·9	328	0·007	-28	12·0	17·5	39·9	69·5	60·0											22/8	
												0·076	-0·144	8·27	379·6	31·5	274·5	0·005		11·0	18·8	39·0	68·9	59·4	-1·0		0·056	6·3							
347	SEA11: 5·44	0·55	37	8·75	0·92	57·74	43·71	75·8	0·740	0·644	77·99	0·093	-0·10	14·5	389·2	43·2	210·8	0·005	-53	12·2	15·8	30·2	58·2	74·6											22/8	
												0·076	-0·069	12·06	568·5	35·5	405·2	0·005		8·7	13·1	35·1	56·9	72·9	-2·2		0·056	6·3							
																			Σpvc	+131															
292	SEA27: 3·78	1·93	5	10·31	0·92	68·84	46·14	67·0	0·871	0·678	91·89	0·058	-0·033	8·040	350·8	34·99	300·0	0·006	-151	10·6	18·9	33·5	63·1	68·6											22/8	Interim, but distant from set of 10
												0·076	-0·113	9·522	497·0	33·14	350·8	0·005		8·5	15·0	38·5	62·0	67·5	-1·7		0·056	6·3							
268	SEA02: 5·05	0·55	42	7·60	0·67	30·23	21·64	71·6	0·692	0·480	35·92	0·094	-0·061	10·9	536·8	26·4	600·0	0·008	+62	4·0	5·6	17·1	26·8	74·6											22/8	
												0·076	-0·062	9·69	663·7	31·3	452·8	0·006		4·0	6·7	17·5	28·2	78·5	+5·2		0·056	6·3							
336	SEA42: 3·80	0·83	15	12·58	1·30	116·90	63·02	37·8	1·063	0·971	223·87	0·090	-0·096	8·23	128·8	43·8	127·7	0·005	+58	22·0	43·1	37·9	103·0	46·0											23/8	
												0·076	-0·140	7·37	132·3	34·4	118·6	0·005		23·8	43·3	37·0	104·1	46·5	+1·1		0·056	6·3							
220	SEA36: 2·78	1·1	19	11·72	0·83	63·8	38·54	60·4	0·991	0·616	85·02	0·087	-0·147	6·88	289·6	27·12	207·6	0·003	-123	10·2	17·1	26·6	53·9	63·4											23/8	
												0·076	-0·173	6·99	401·8	27·7	285·7	0·005		7·4	14·4	30·6	52·3	61·6	-2·9		0·056	6·3							
241	SEA29: 2·19	1·1	40	10·83	0·54	25·13	16·65	66·3	0·915	0·397	32·25	0·088	-0·226	-3·19	575	11·20	300·0	0·005	+42	1·3	5·3	19·2	25·9	77·8											23/8	
												0·076	-0·175	1·30	592·9	24·24	394·9	0·005		2·4	5·2	18·8	26·5	79·6	+2·3		0·056	6·3							
																			Σpvc	-112															

Table III: Optimised and predicted coefficients in the selected seas.

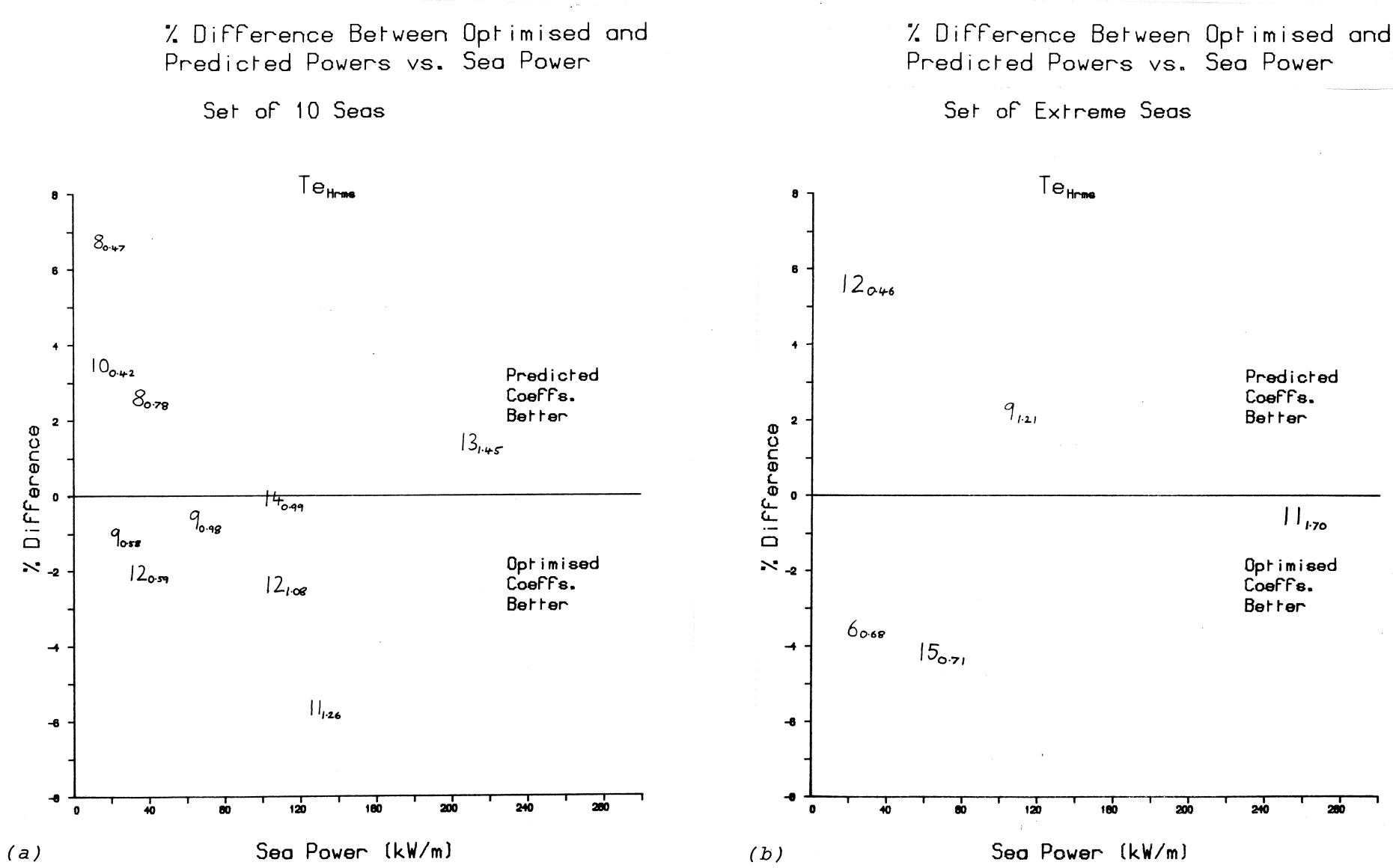

Figure 9: Percentage difference between optimised and predicted powers vs. sea power for each set.

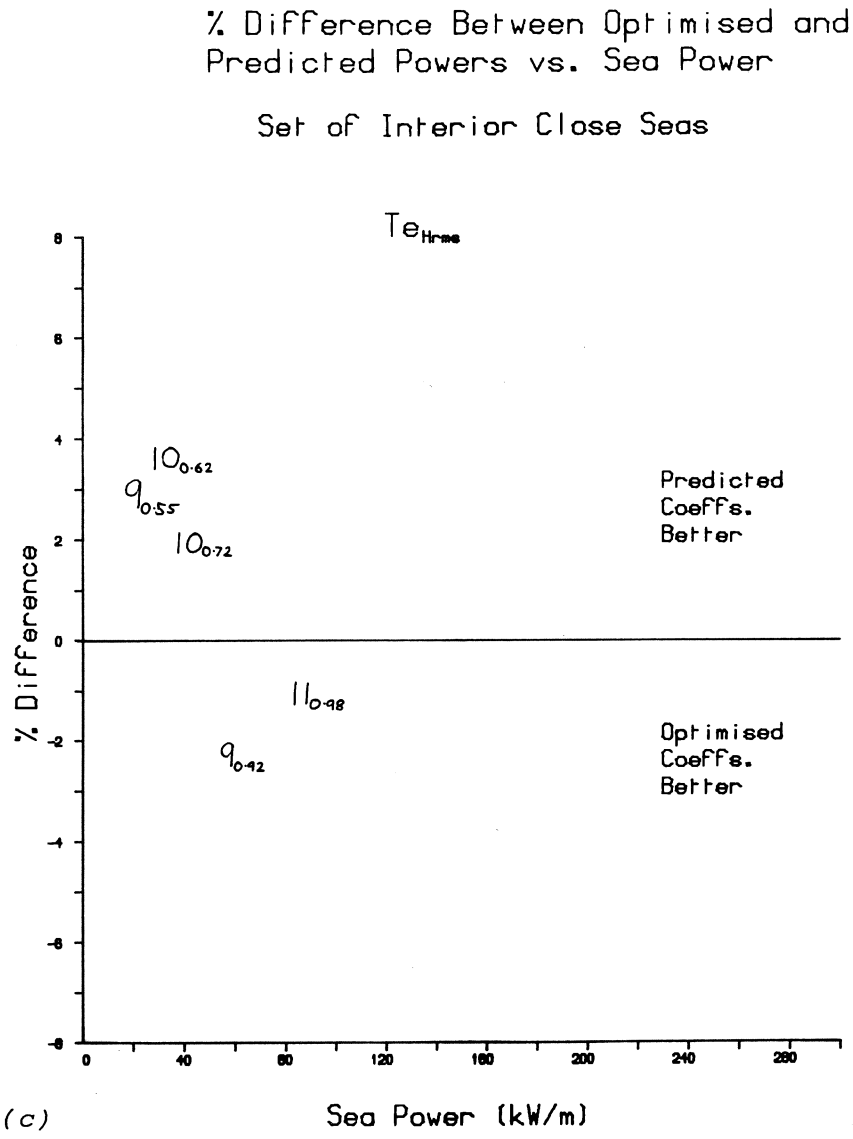

(c)

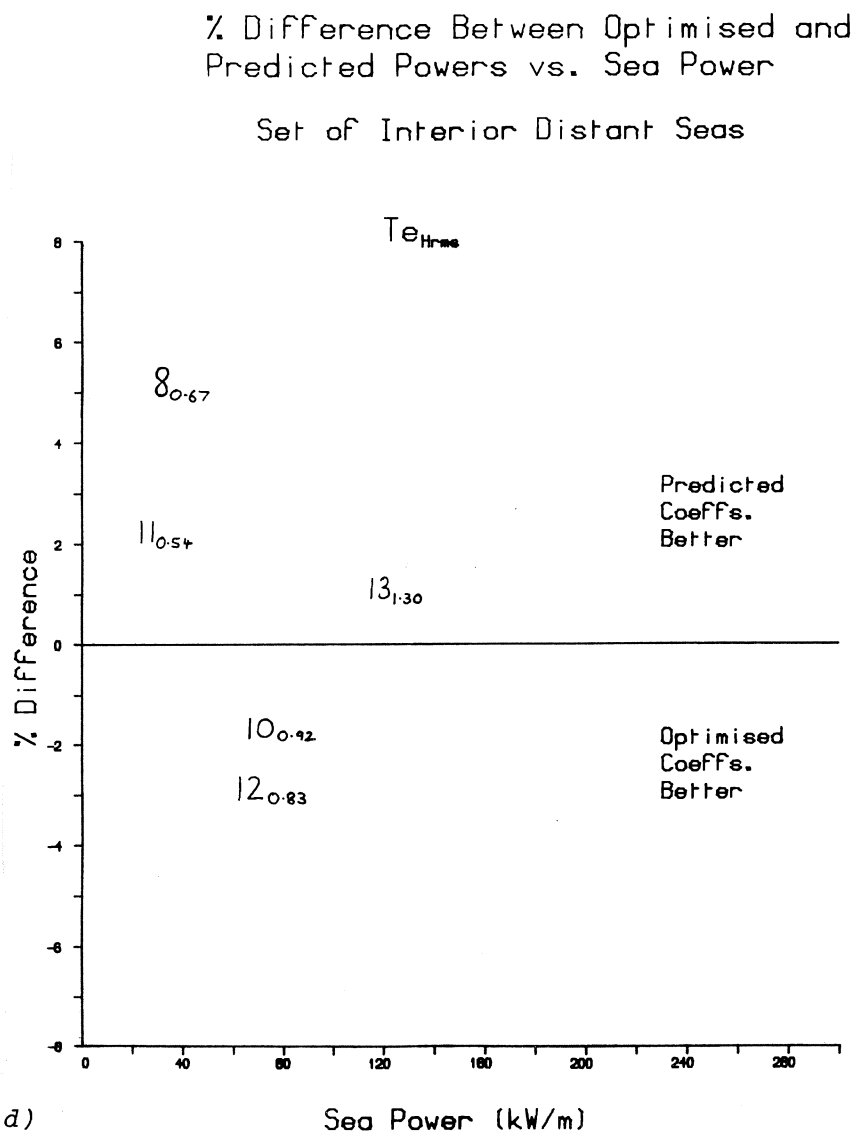

(d)

Figure 9: Percentage difference between optimised and predicted powers vs. sea power for each set.

Future Work

There are plans to investigate the effects of other non-linear control coefficients (eg θ^2 , S x H, H^2 x θ etc), and develop a more complex non-linear power take-off strategy to increase duck performance further. This work should, however, have a strong theoretical base, since empirically testing the effects of every conceivable coefficient would take rather a long time.

At present, work is being carried out to develop a more efficient simplex optimisation program, and it is hoped that this will be used in the development of both spine mounted ducks and solo ducks in the Wide and Narrow Tanks.

Acknowledgements

The Narrow Tank and associated facilities were developed with the help of a grant from the Department of Energy. Thanks are due to David Jeffrey for carrying out much of the hardware and software development, Stephen Salter who helped to keep the experiment running over the two month period and Fiona Donaldson for providing the graphs in the main part of the report.

References

1. Mynett, A.E., Serman, D.D. and Mei, C.C., 'Characteristics of Salter's Cam for Extracting Energy from Ocean Waves', Appl. Ocean Res., 1979, vol 1, p.13.

2. Edinburgh Wave Power Project 4th year Report, Section 6.

3. Crabb, J.A., 'Selected Directional Wave Spectra for Use in the Assessment of Wave Energy Convertor Performance', Institute of Oceanographic Sciences, Internal Document 131, 1981, Taunton.

4. Rendell, Palmer and Tritton, Working Paper 42.

5. Edinburgh Wave Power Project 2nd Year Report, Section 26.15

6. Edinburgh Wave Power Project 2nd Year Report, Section 22.

7. Edinburgh Wave Power Project 4th Year Report, Section 4.

8. Evans, D.V., Jeffrey, D.C., Salter S.H., and Taylor, J.R.M., 'Submerged Cylinder Wave Energy Device: Theory and Experiment', Appl. Ocean Res., 1979, Vol 1, pp3-12.

9. Mollison, D., 'Productivity Analysis of Salter Ducks', updated report on the Edinburgh-Laing Wave Energy Device, October 1981, Sect. 7.1, pp 177-192.

10. Updated Report on the Edinburgh-Laing Wave Energy Device, October 1981, Section 10, Drawing No 10071.

11. Himmelblau, D.M., 'Applied Nonlinear Programming', McGraw-Hill 1972, Section 4.2.

Appendix A: Narrow Tank Control System

Figure A.1 shows a block diagram of the relevant narrow tank instrumentation. A Sirius microcomputer running the UCSD operating system and programmed in PASCAL is the narrow tank system controller. It is able to store data on floppy discs, or output it to a printer and a plotter. Its main task was to measure the three sets of force and velocity signals for a 90 second period at a rate of 20Hz. It was then able to calculate the power extracted in each of the three degrees of freedom by multiplying the force and velocity time series.

The command signals to the duck and its mounting were calculated by a PET microcomputer on the basis of the velocity and displacement signals in each of the three modes. The PET was programmed in FORTH to sample the six signals, calculate the three drive signals, and update the outputs to the duck and its mounting at a rate of about 50Hz, while also controlling the wavemaker as an interrupt driven background task.

The 'Zoo Keeper' switch box has two main functions. Firstly, it monitors all the drive signals to the duck, its mounting and the wavemaker, so that in the event of a malfunction causing a dangerously large drive signal, it can prevent them from being damaged by disconnecting them from the faulty equipment. This proved to be a useful safeguard when the system was left running overnight or at weekends. Secondly, it allows the user to drive the duck and its mounting from either the normal manual model controls, or a 12 bit digital to analogue convertor (which was not used in this series of experiments) or the PET's duck controller outputs.

As shown on the left of Figure A.1, the PET, which is normally connected as a 'slave' to the Sirius via the General Purpose Interface Bus (GPIB), can also access its own printer and floppy disc drives on its own private GPIB.

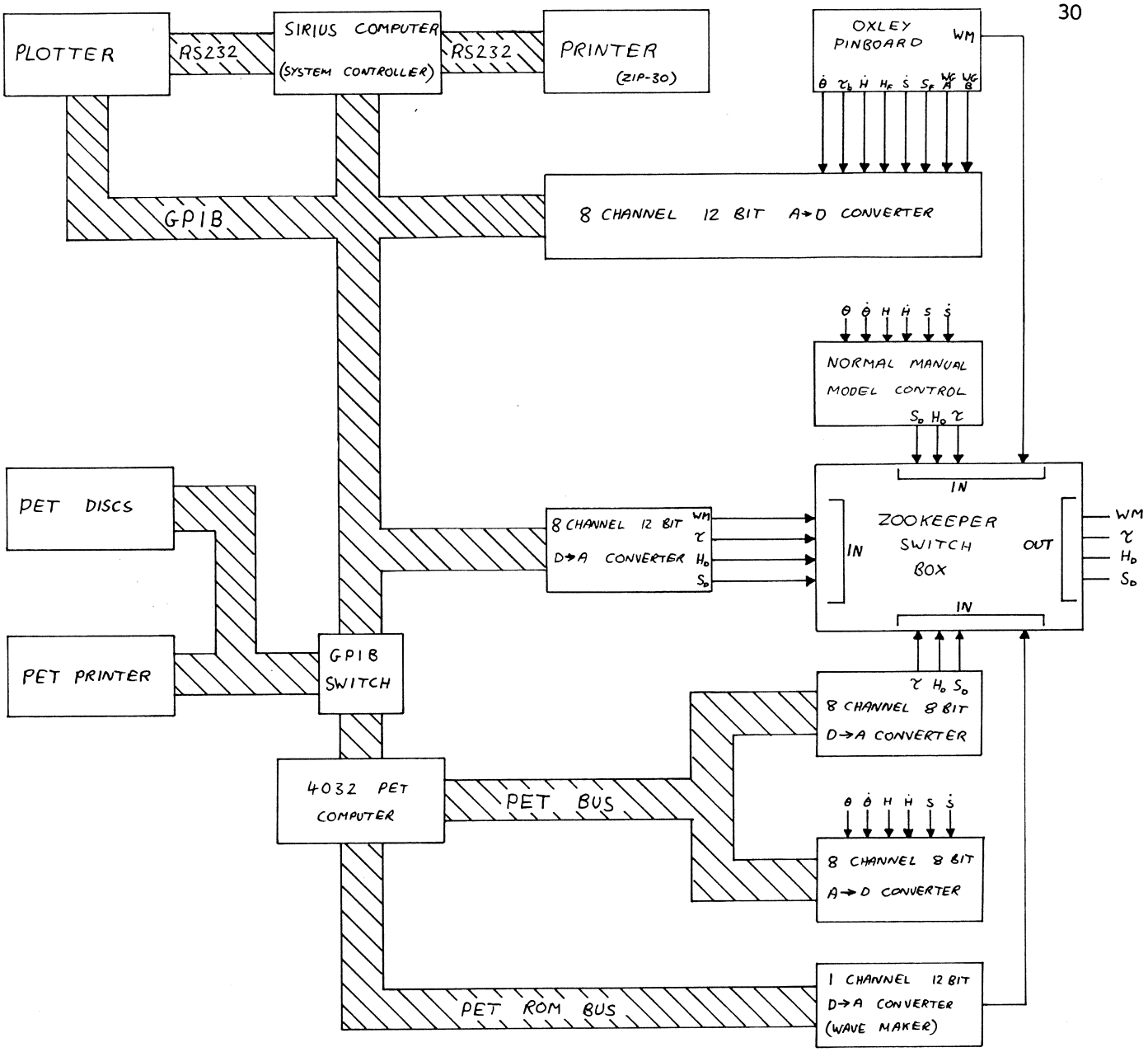

WM - Wavemaker Drive
τ - Torque Drive
H - Heave Drive
S - Surge Drive

θ - Angular Displacement
θ - Angular Velocity
τ - Measured Torque
S - Surge Displacement
S - Surge Velocity
S - Surge Force
H - Heave Displacement
H - Heave Velocity
H - Heave Force

Figure A.1: Narrow Tank Block Diagram.

Appendix B: An Explanation of How to Read Tables 1(a) and 1(b)

The two tables show the results of optimisations carried out in 46 different seas, a few of which were repeated. The tables consist of 36 columns, some of which are grouped under headings. The following is an explanation of the significance of each column.

SEA DATA

SEA # — The Institute of Oceanographical Sciences (IOS) spectrum number.

SEA NAME — Name of sea as recognised by the PET microcomputer. The format is SEAxx:y.yy, where xx is a number between 1 and 46 ordering the seas by their Te Value, and y.yy refers to the manual potentiometer setting required to achieve the correct Hrms.

MARTIN EQUIV — Refers to the 'most similar' sea used by Martin Greenhow in his manual optimisation experiments. His optimised coefficients were used as the starting point in each of the automatic optimisations. His sea name format was xxxRyyy where xxx is 100 x Te at full scale, and yyy is 100 x Hrms (m) at full scale. It should be noted that his experiments were carried out at a scale of 1:100, not 1:140, and that wavelength/duck diameter and wave height/-duck diameter ratios should be preserved when changing scale.

WEIGHT — Is the % of the annual wave climate off South Uist represented by this sea[9]. Note that the sum of all 46 weights is 100%.

RATING — The seas are ranked according to duck productivity (Weight x PLTD) with the most important sea having a rating of 1.

FULL SCALE

Te — The full-scale Te of the sea[3].

Hrms — The full-scale Hrms of the sea[3].

Psea — The full-scale power in the sea per unit length of wave front.

Pltd — The maximum power that can potentially be extracted by the Nov '81 reference design.[9] This figure accounts for the electrical and hydraulic losses in the front-end power extraction system, and the 63.02 kW/m power limit.

Nov '81 — The efficiency of the reference design [9] based on Martin Greenhow's optimum linear control strategy (1980).

TANK SCALE

Tank scale is 1:140
Appendix B contains a note on how various parameters scale.

Te — The tank scale Te of the sea

D. CORR Hrms — The depth corrected Hrms of the sea at tank scale. In order to obtain this figure, the full-scale Hrms has to be scaled down, and the depth correction for the Te value applied (see Figure 3).

Psea — Is the power in the sea at the model position corrected to the tank width of 31.1 cm.

COEFFICIENTS

These are the seven duck coefficients:

DDC	Duck (nod) Damping Coefficient
DSC	Duck (nod) Spring Coefficient
HDC	Heave Damping Coefficient
HSC	Heave Spring Coefficient
SDC	Surge Damping Coefficient
SSC	Surge Spring Coefficient
VDC	Velocity Displacement Coefficient

In each case, the top figure is the manually optimised value found by Martin Greenhow, used as the initial value in the automatic optimisation, and the bottom figure is the final optimised value.

TEST NUMBER

The experiments were numbered sequentially in chronological order, except for those which were repeats of earlier tests.

POWERS

These are the initial and final powers in each of the three modes together with the total power extracted.

MISC 1

η	The initial and final efficiencies.
CHANGE	The percentage change in efficiency achieved by the optimisation.
# RUNS	The number of times that the tank was run (for 90 seconds) during the course of the optimisations. Each tank run took about 4 minutes (90s for sampling and 150s for the power calculation)..

TORQUE LIMIT The limit applied to the torque drive signal at tank scale.

HUB DEPTH The distance between the duck's equilibrium hub position, and the mean water level at tank scale.

Hrms FRONT/REAR

The Hrms wave height one metre either side of the model.

OFFSETS

NOD TORQUE OFFSET The average of the measured torque over the 90s sampling period. This should be zero, and in all cases was found to be so to within the accuracy of the system.

HEAVE FORCE OFFSET This is a measure of the negative sinking force on the duck since heave force is positive upwards.

SURGE FORCE OFFSET This is a measure of the mooring force on the duck. Surge force is positive in the direction in which the waves travel (towards the beach).

MISC 2

DATE When the experiment was started. It usually finished the following morning, or after a weekend.

COMMENTS Relevant comments about any unique features of the experiment.

Appendix C: A Note on Scale

Dynamic similarity exists between model and prototype. One can convert full-scale figures into model figures and vice versa by use of the appropriate scaling factor. This is best described by an index of scale.

PARAMETER	INDEX OF SCALE
Lengths	1
Period	0.5
Frequency	-0.5
Angle	0
Angular Velocity	-0.5
Angular acceleration	-1
Force	3
Torque	4
Power	3.5
Power per unit length	2.5
Force per unit length	2
Torque per unit length	3
Mass	3
Inertia per unit length	4
Linear velocity	0.5
Linear acceleration	0

Appendix D: Duck Control Coefficient Plots

This appendix consists of scatter diagrams showing the dependance of the optimised duck control coefficients on Te and Hrms.

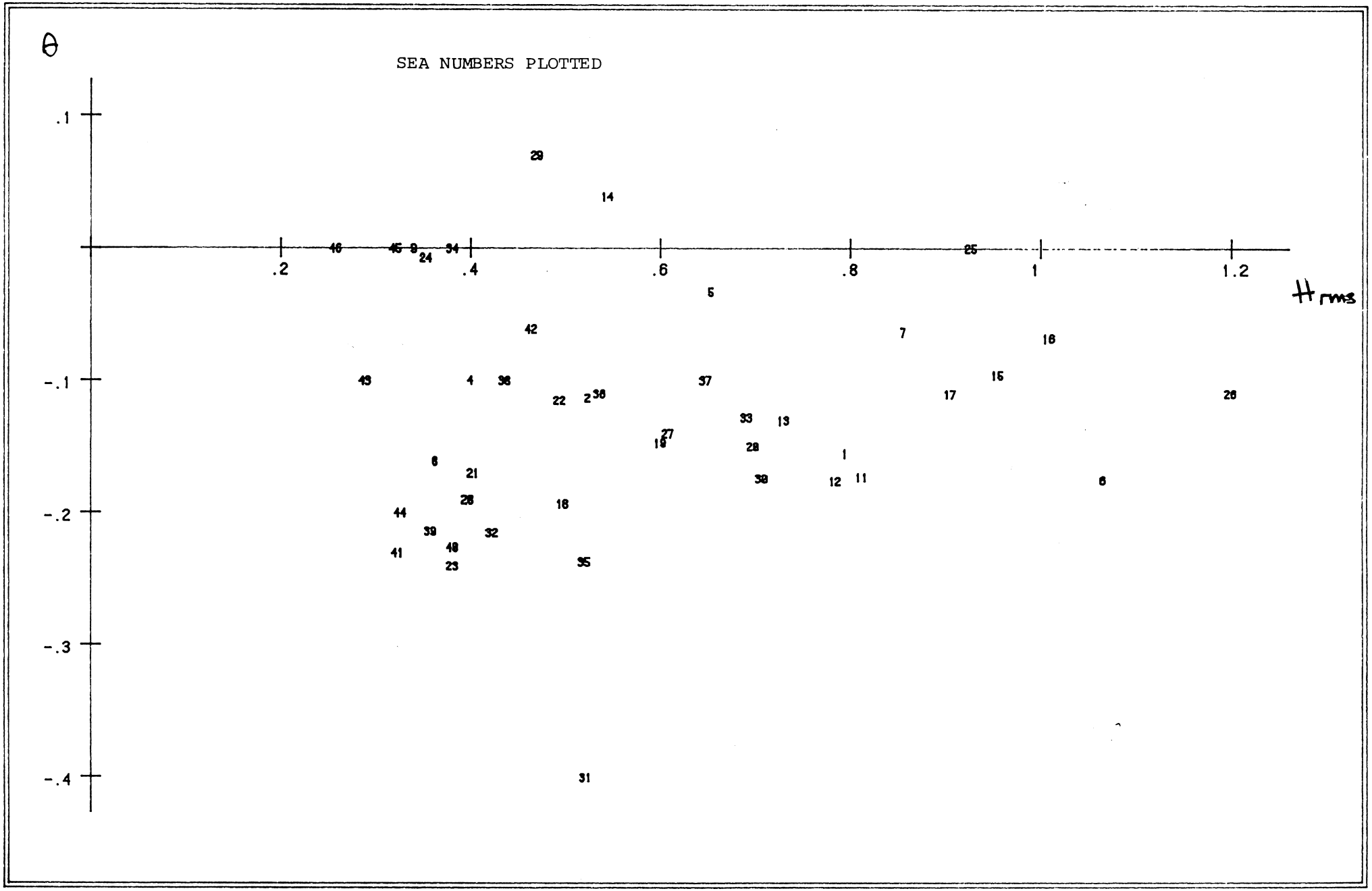
θ
SEA NUMBERS PLOTTED
.1
-.1
-.2
-.3
-.4
.2
.4
.6
.8
1
1.2
Hrms
29
14
46
45
9
24
34
25
5
42
7
16
49
4
38
37
15
22
2
36
17
26
33
13
27
18
28
1
6
21
39
12
11
6
28
44
18
39
32
41
48
23
35
31

Figure D.1

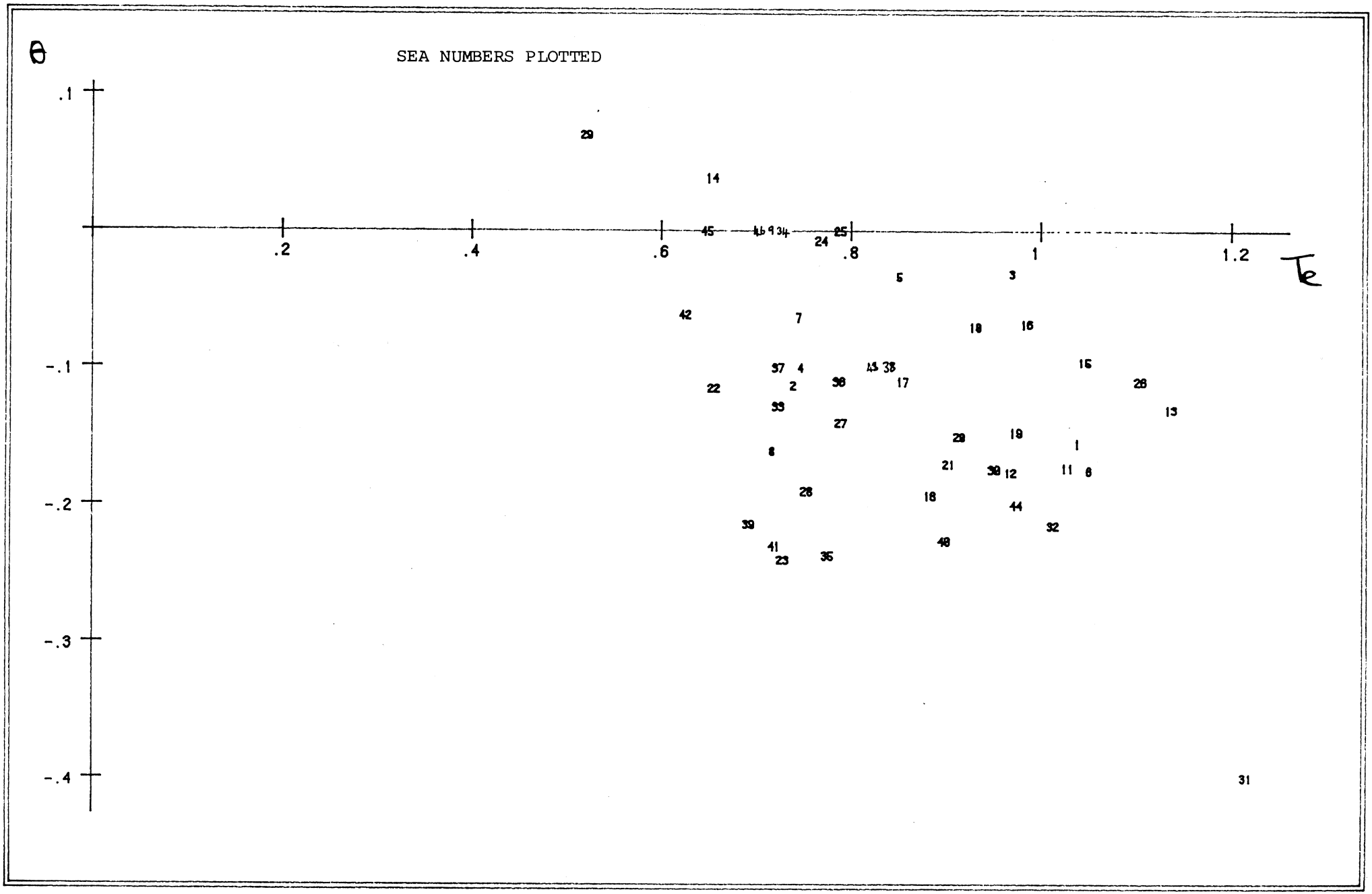
θ
SEA NUMBERS PLOTTED
.1
-.1
-.2
-.3
-.4
.2
.4
.6
.8
1
1.2
Te
29
14
45
46 9 34
24
25
5
3
42
7
18
16
37 4
43 38
15
22
2
36
17
26
33
13
27
28
19
1
8
21
39 12
11
6
26
18
44
39
32
41
23
35
48
31

Figure D.2

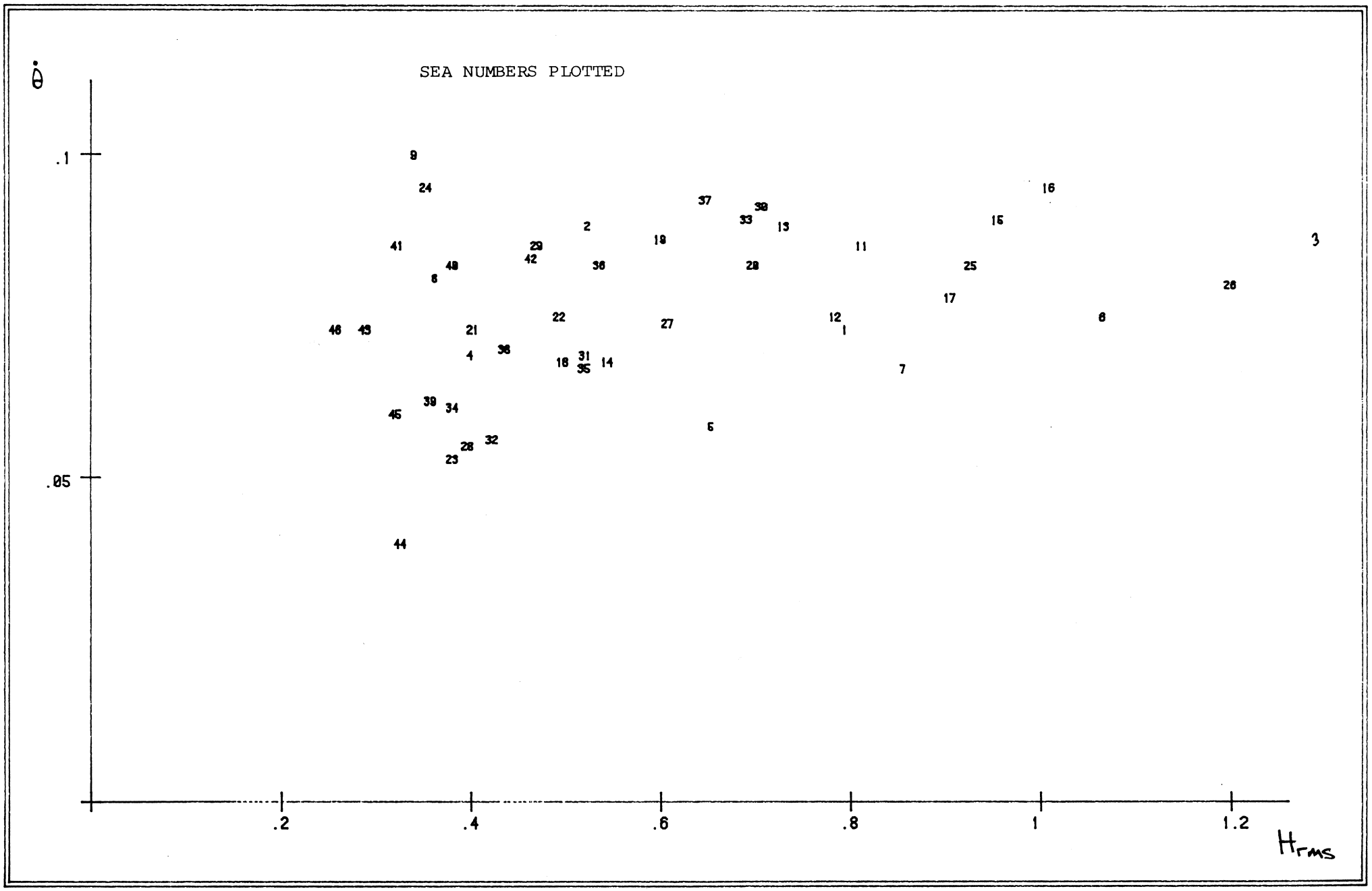
SEA NUMBERS PLOTTED
θ̇
.1
.05
9
24
37
38
33
13
16
15
2
19
3
41
29
42
11
49
36
28
25
6
26
17
22
12
8
46
45
21
27
1
4
36
31
35
18
14
7
39
34
45
5
28
32
23
44
.2
.4
.6
.8
1
1.2
Hrms

Figure D.3

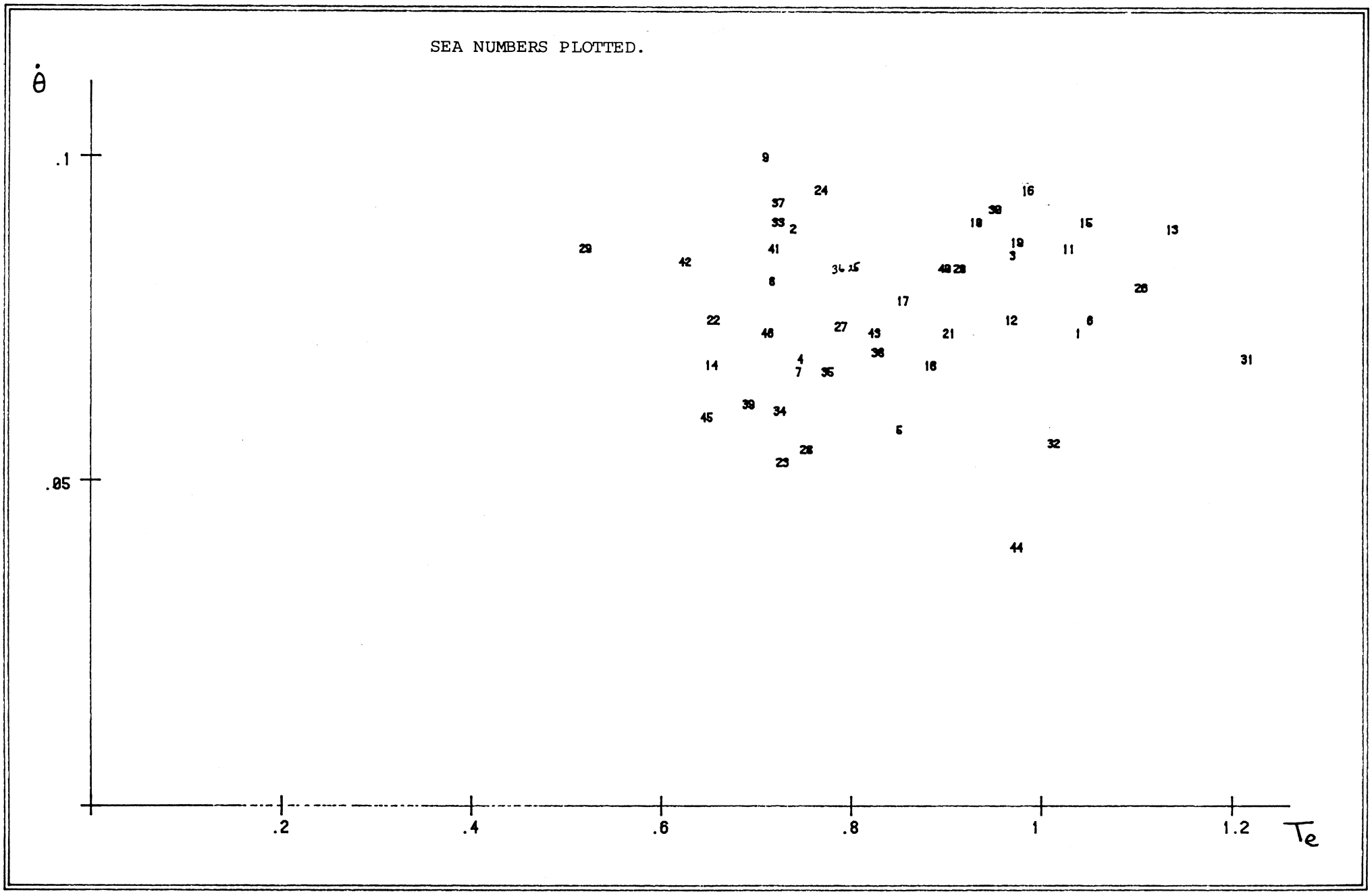

Figure D.4

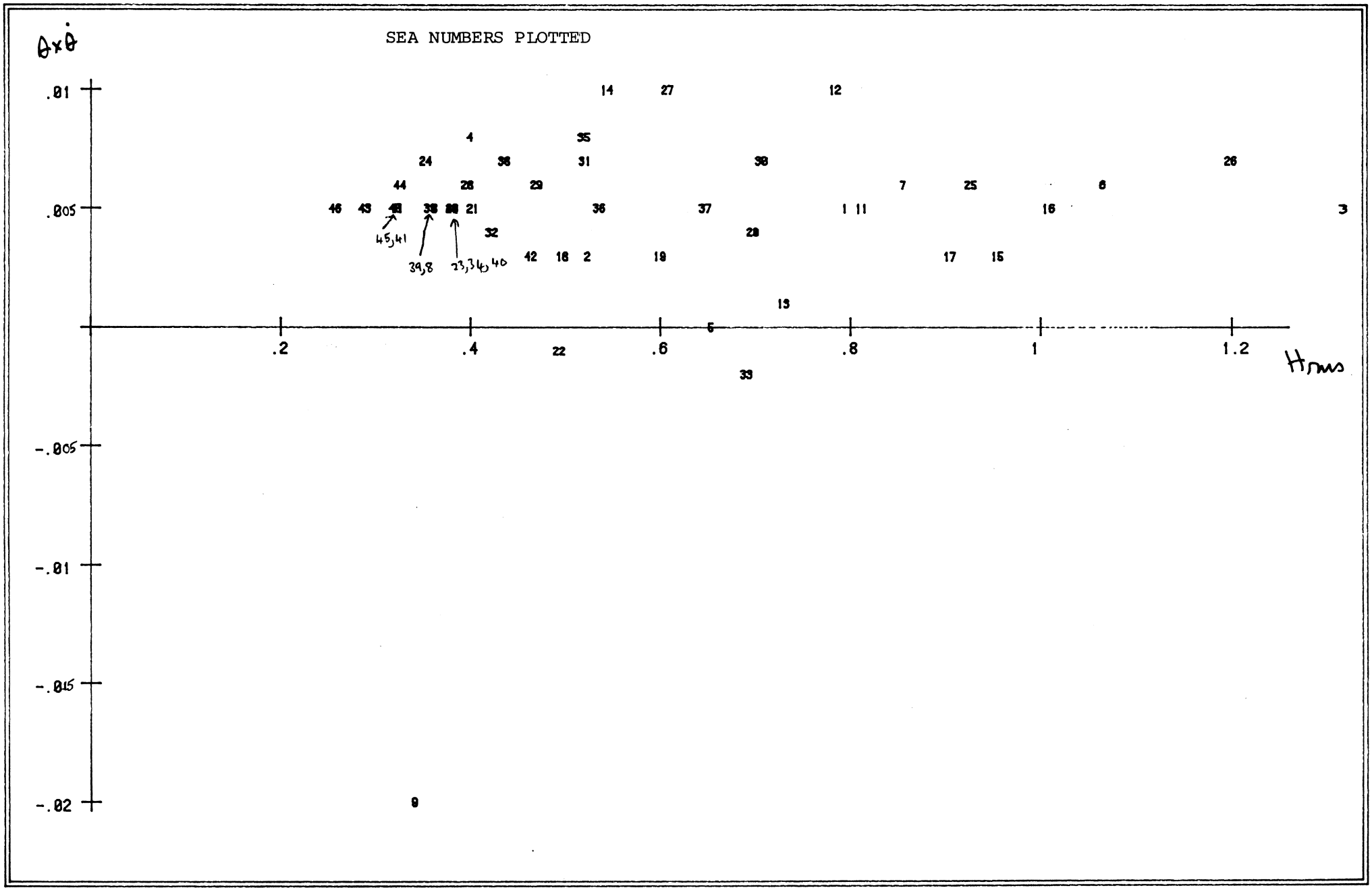
SEA NUMBERS PLOTTED
θxθ̇
.01
.005
-.005
-.01
-.015
-.02
.2
.4
.6
.8
1
1.2
Hrms
14 27 12
4 35
24 36 31 38 26
44 28 29 7 25 6
46 43 45 41 39 8 23 34 40 21 36 37 1 11 16 3
32 28
42 18 2 19 17 15
13
5
22
33
9

Figure D.5

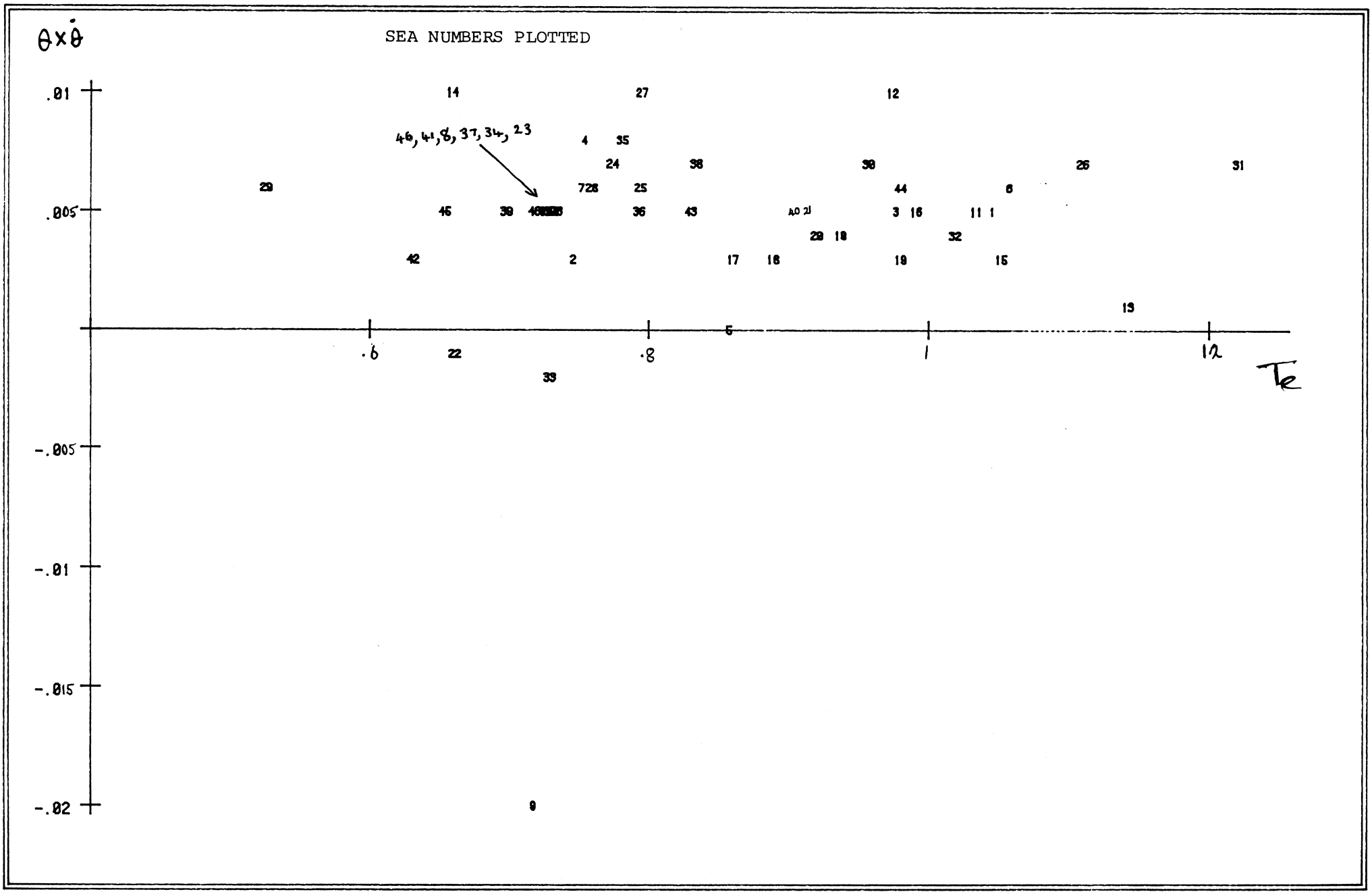
θxθ̇
SEA NUMBERS PLOTTED
.01
.005
-.005
-.01
-.015
-.02
.6
.8
1
1.2
Tε
46, 41, 8, 37, 34, 23

Figure D.6

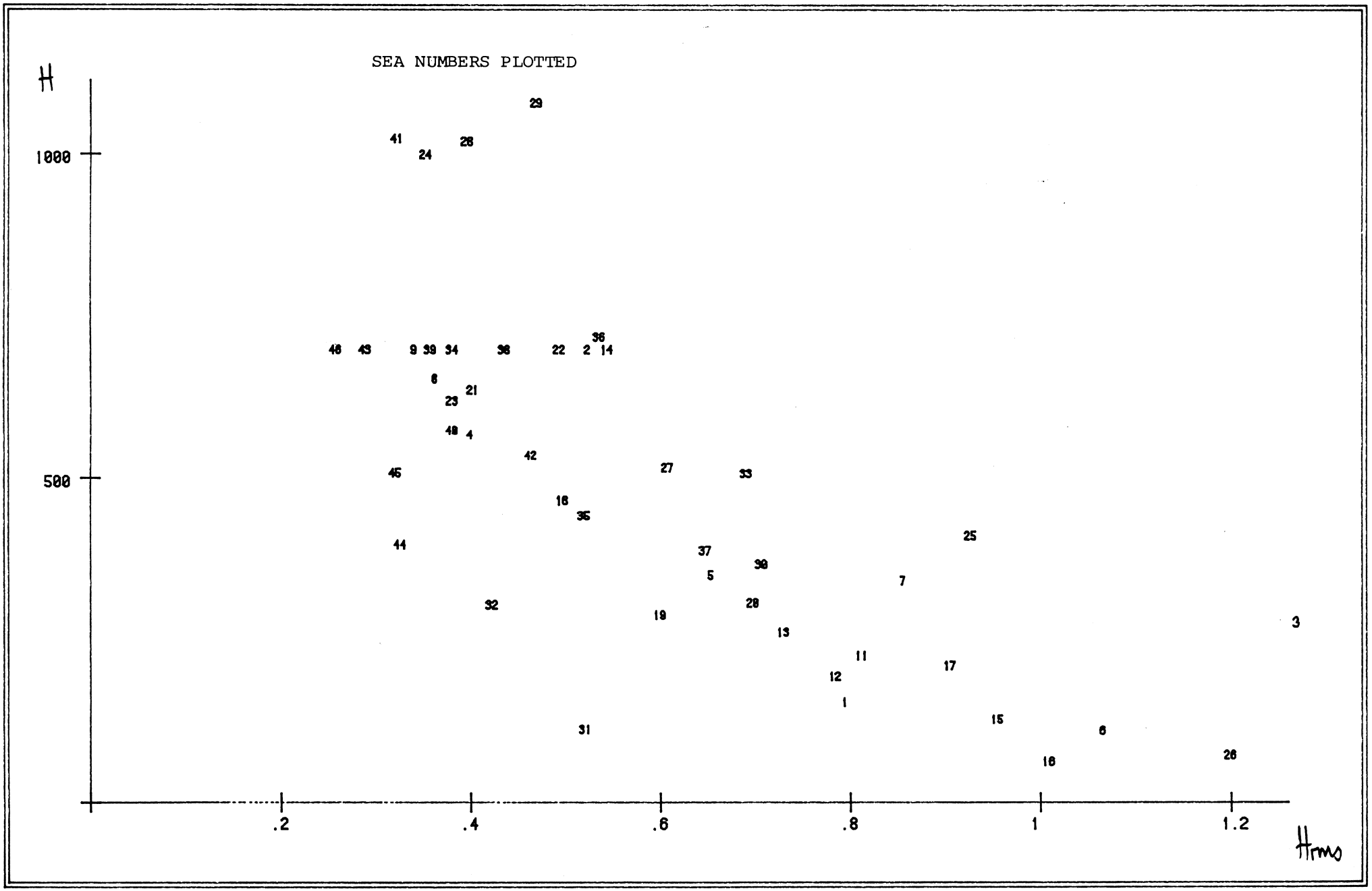
SEA NUMBERS PLOTTED
#
1000
500
.2
.4
.6
.8
1
1.2
Hrms
29
41
28
24
36
46
43
9
39
34
38
22
2
14
6
21
23
48
4
42
45
27
33
18
35
44
25
37
38
5
7
32
28
19
3
13
11
17
12
1
15
31
6
16
26

Figure D.7

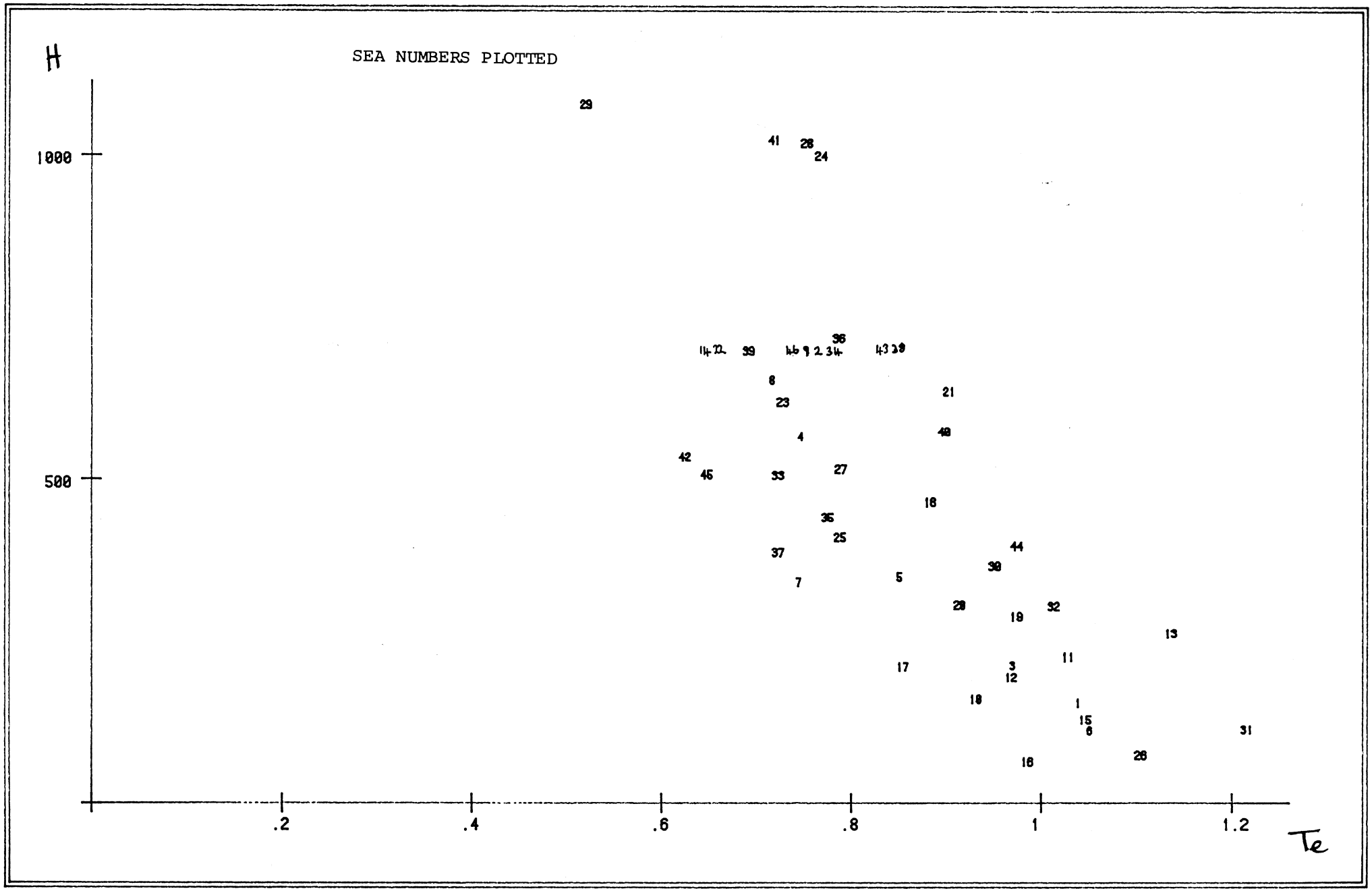

Figure D.8

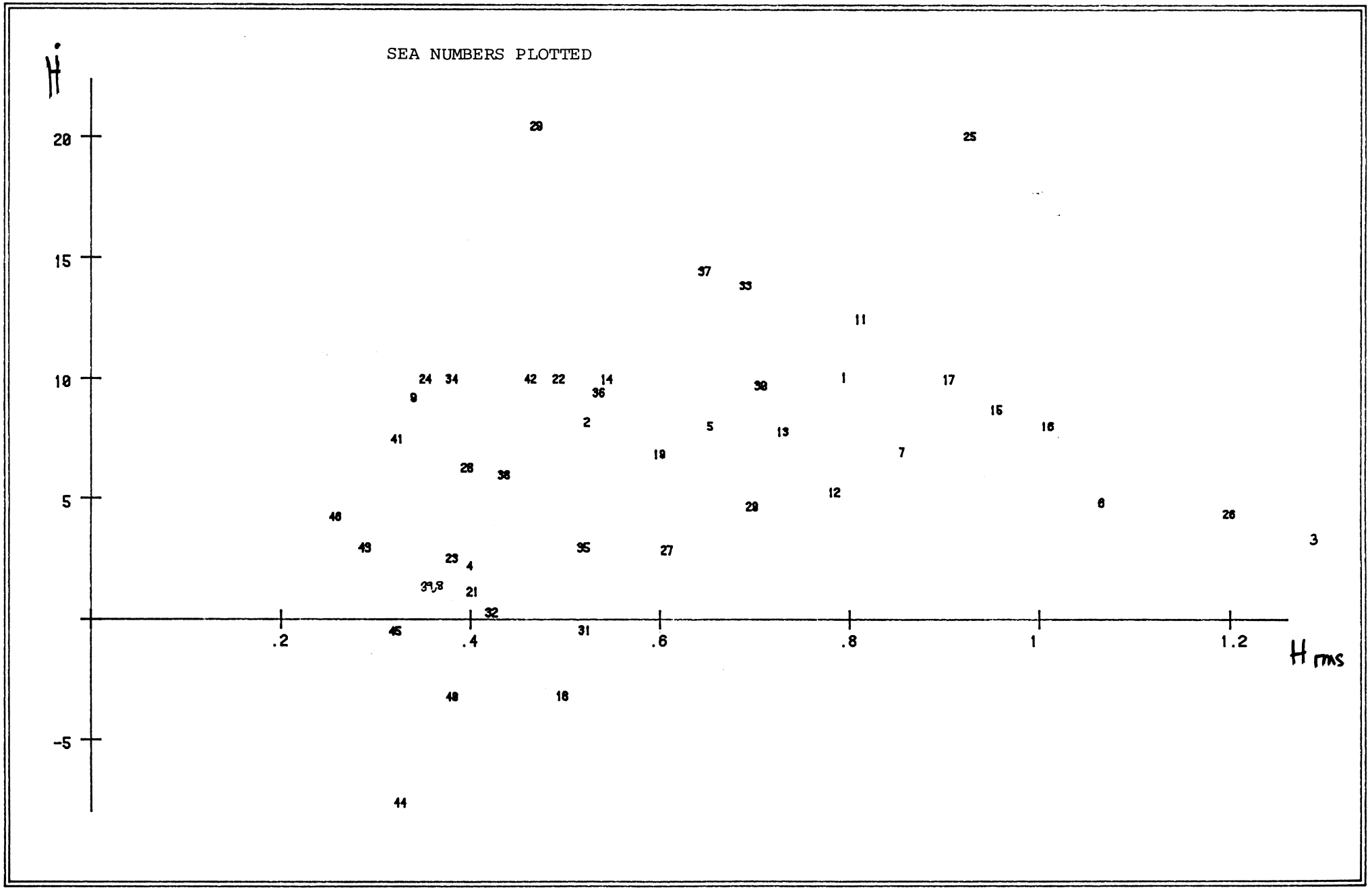
SEA NUMBERS PLOTTED
20
15
10
5
-5
.2
.4
.6
.8
1
1.2
H rms
29
25
37
33
11
24
34
42
22
14
36
1
17
9
38
15
2
5
13
16
41
19
7
28
38
12
6
46
29
26
49
35
27
3
23
4
39,8
21
32
45
31
48
18
44

Figure D.9

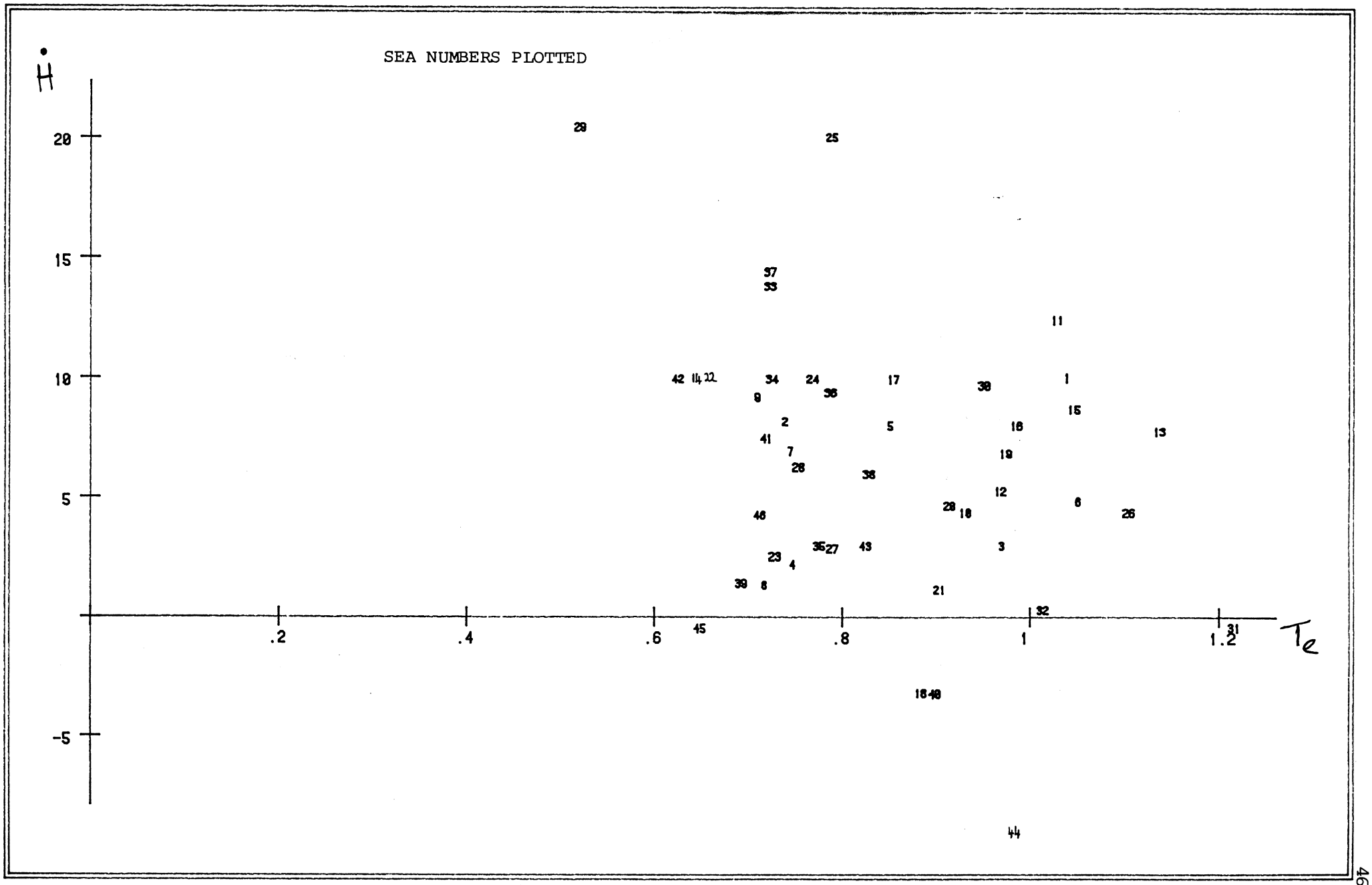
SEA NUMBERS PLOTTED
Ḣ
20
15
10
5
-5
.2
.4
.6
.8
1
1.2
Te
29
25
57
33
11
42 14 22
34
24
17
38
1
9
36
15
2
5
16
13
41
7
19
28
38
12
46
28
18
6
26
35
27
43
3
23
4
39
8
21
32
45
31
18
48
44

Figure D.10

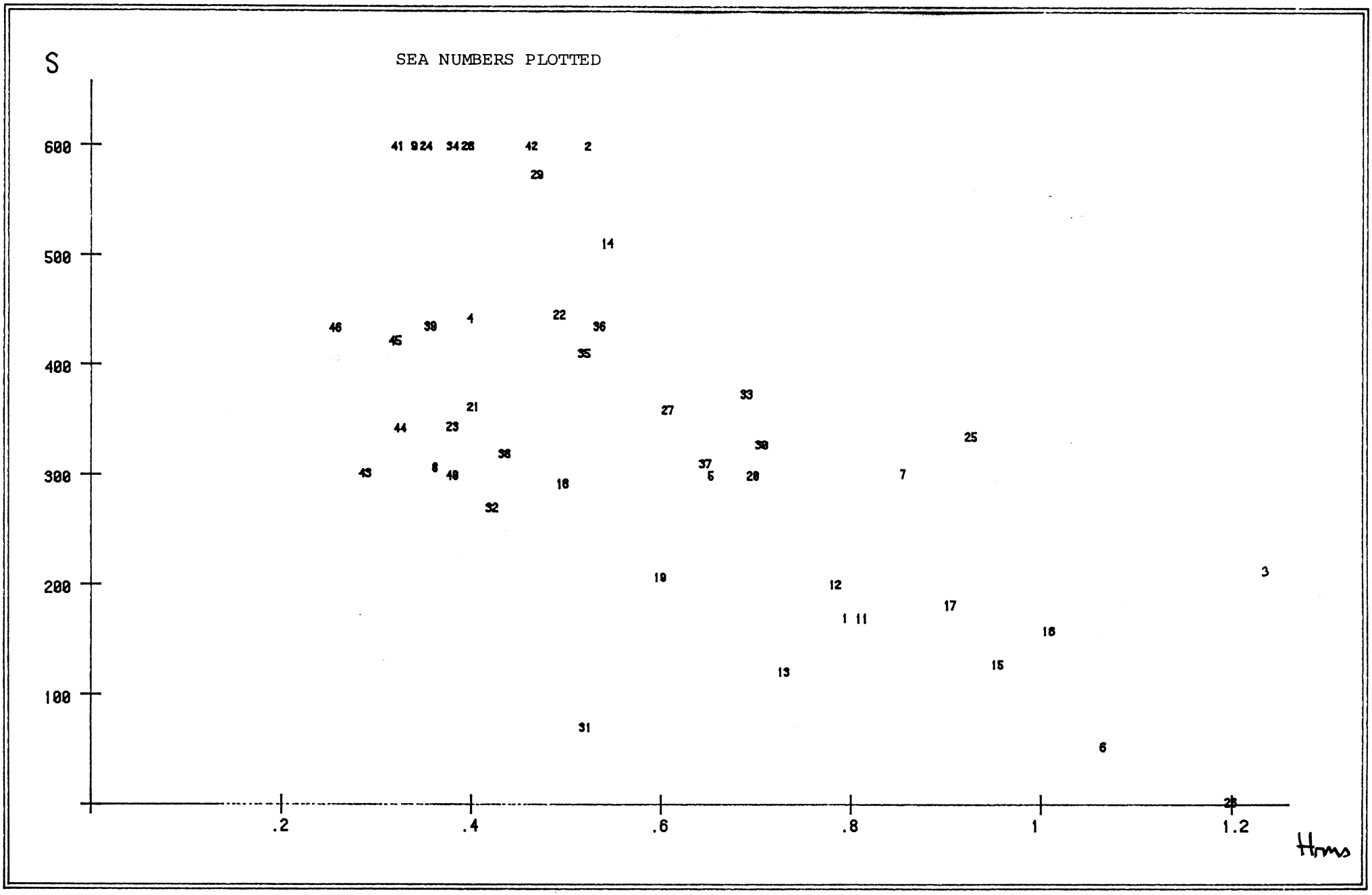
SEA NUMBERS PLOTTED
S
600
500
400
300
200
100
.2
.4
.6
.8
1
1.2
Hrms
41 9 24 34 28
42
2
29
14
46
39
4
22
36
45
35
33
21
27
44
23
25
38
36
37
43
8
48
5
28
7
16
32
19
3
12
17
1 11
18
13
15
31
6

Figure D.11

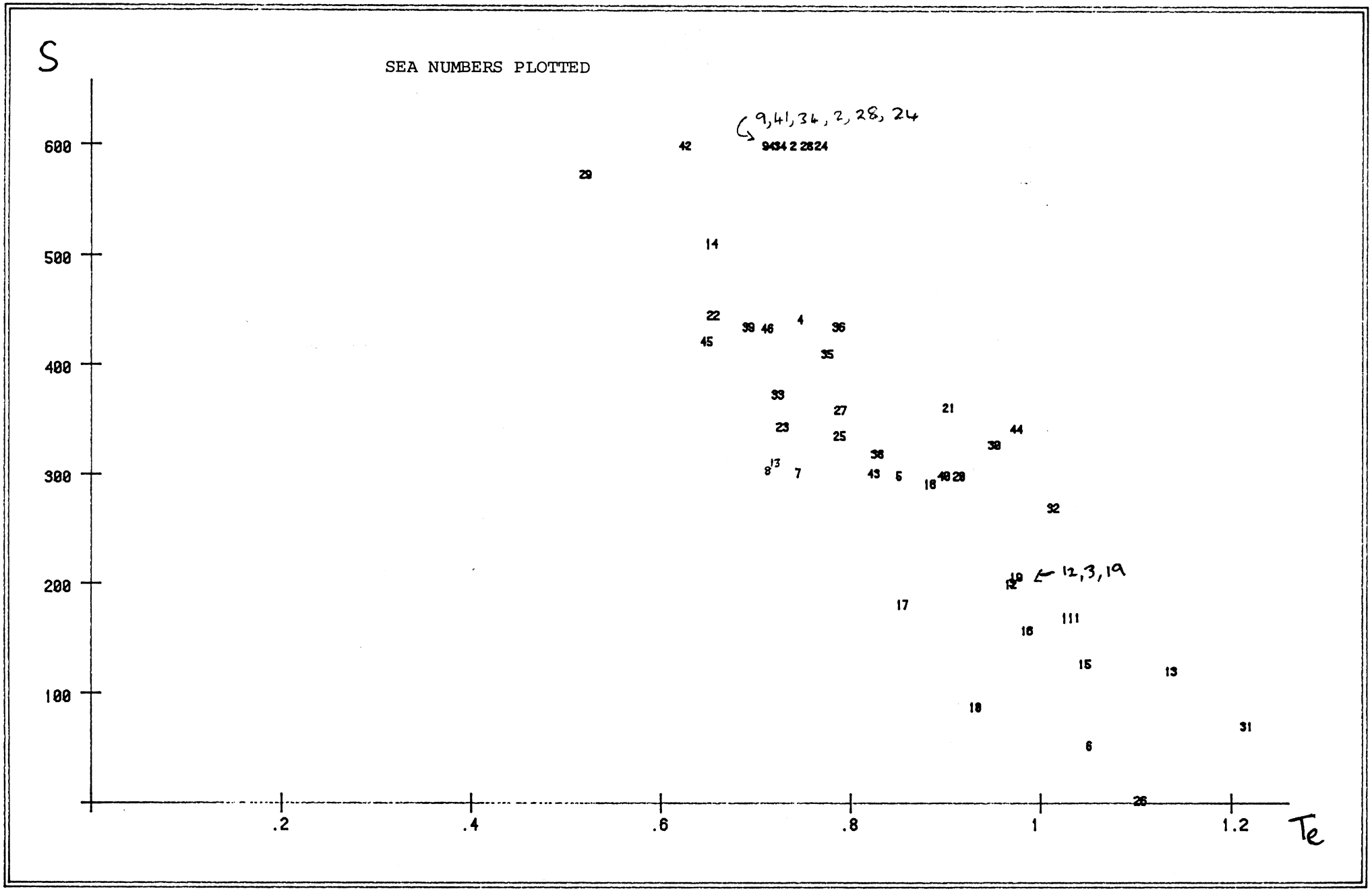
S
SEA NUMBERS PLOTTED
9,41,34,2,28,24
600
500
400
300
200
100
.2
.4
.6
.8
1
1.2
Te
42
9434 2 2824
29
14
22
39 46
4
36
45
35
33
27
21
23
25
44
38
38
8 13
7
43
5
16
40 28
32
12,3,19
17
111
16
15
13
18
31
6
26

Figure D.12

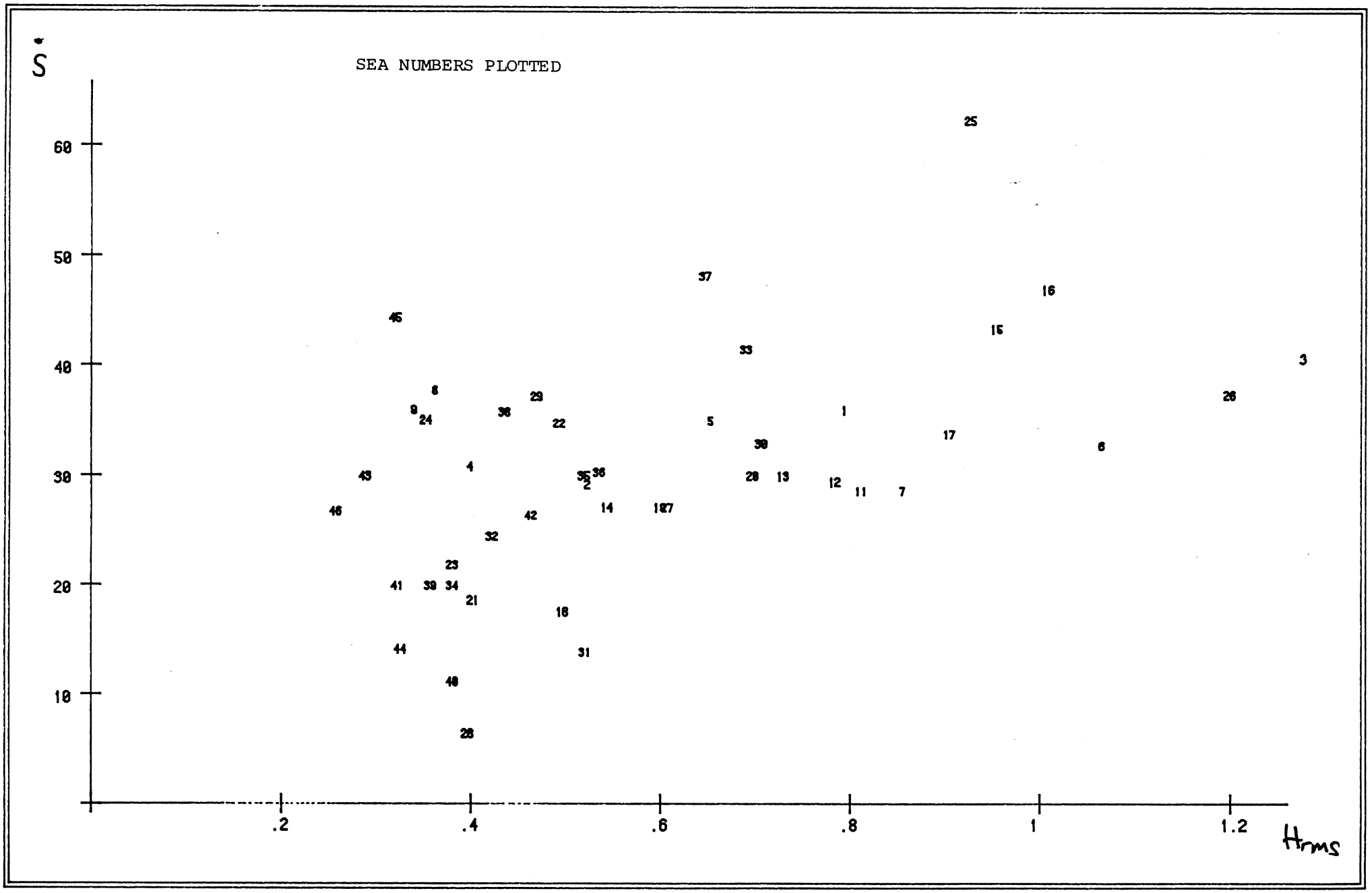
SEA NUMBERS PLOTTED
S
60
50
40
30
20
10
.2
.4
.6
.8
1
1.2
Hrms
25
37
16
45
15
33
3
8
29
26
9
24
36
22
1
5
17
38
6
4
43
35
36
28
13
12
11
7
2
46
14
18
17
42
32
23
41
39
34
21
18
44
31
48
28

Figure D.13

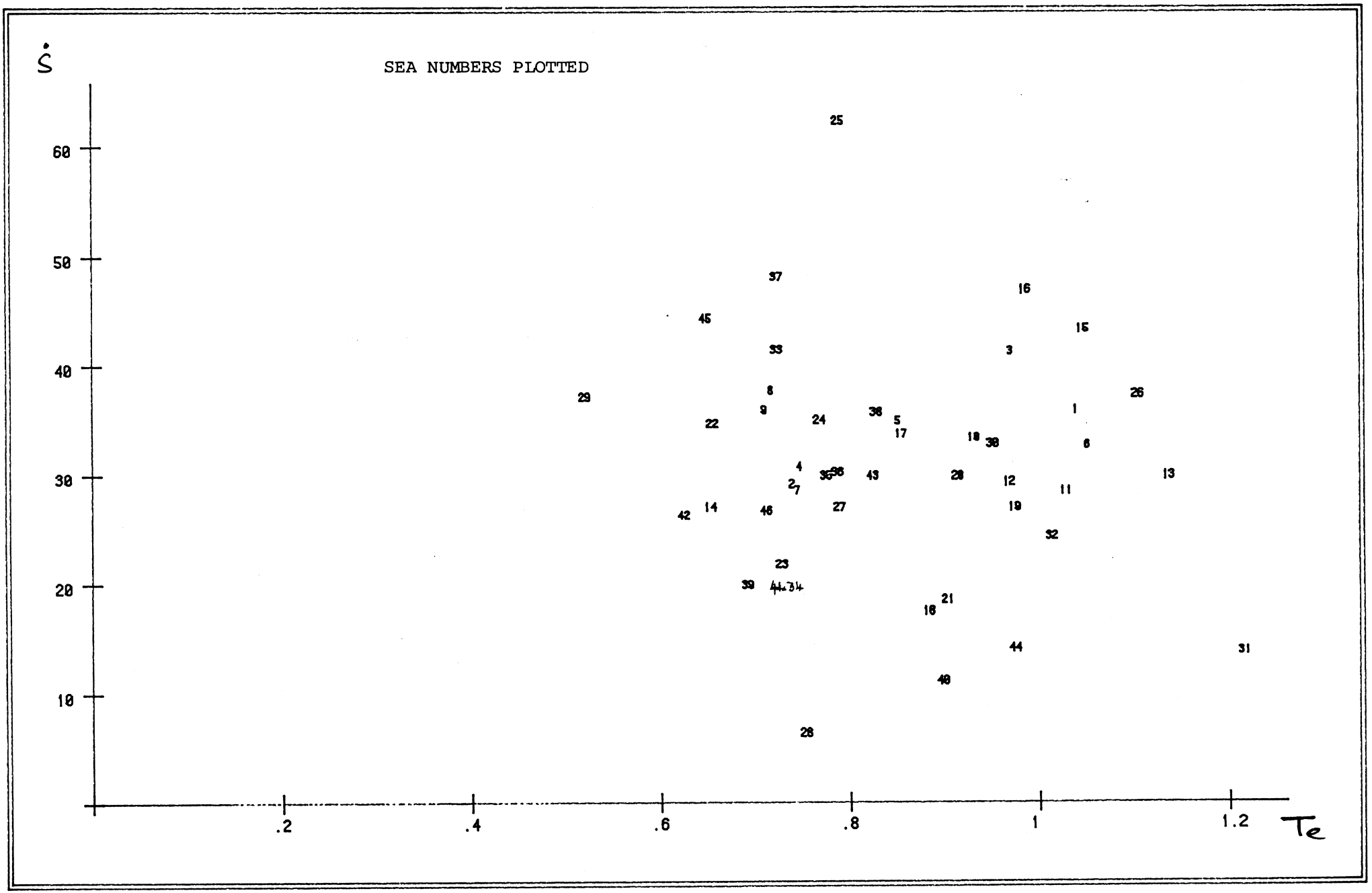
Ṡ
SEA NUMBERS PLOTTED
60
50
40
30
20
10
.2
.4
.6
.8
1
1.2
Te
25
37
16
45
15
33
3
29
8
26
9
1
22
24
38
5
17
18
38
6
4
35
36
43
28
12
13
2
7
11
42
14
46
27
19
32
23
39
44
34
21
18
44
31
40
28

Figure D.14

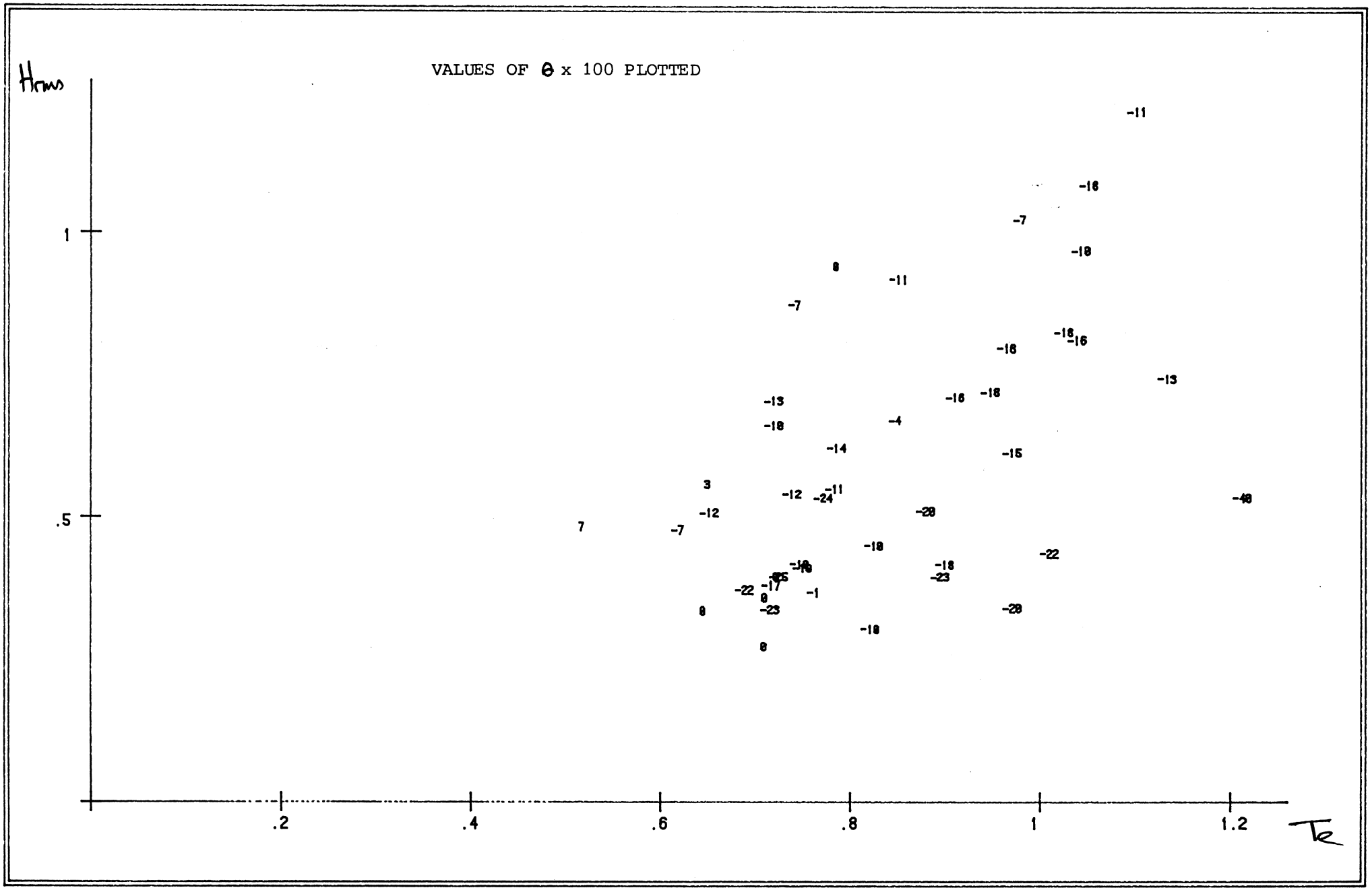

Figure D.15

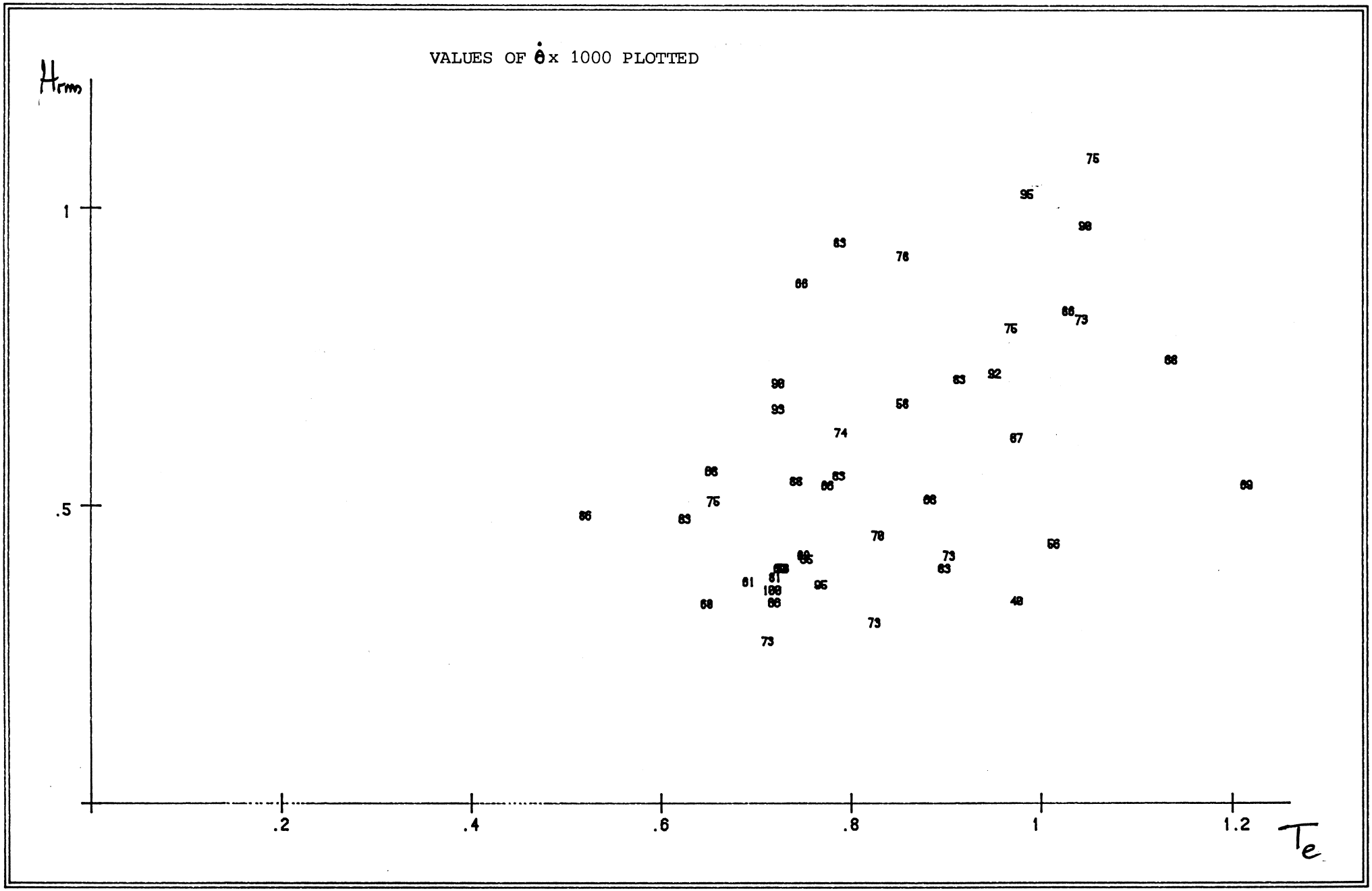

Figure D.16

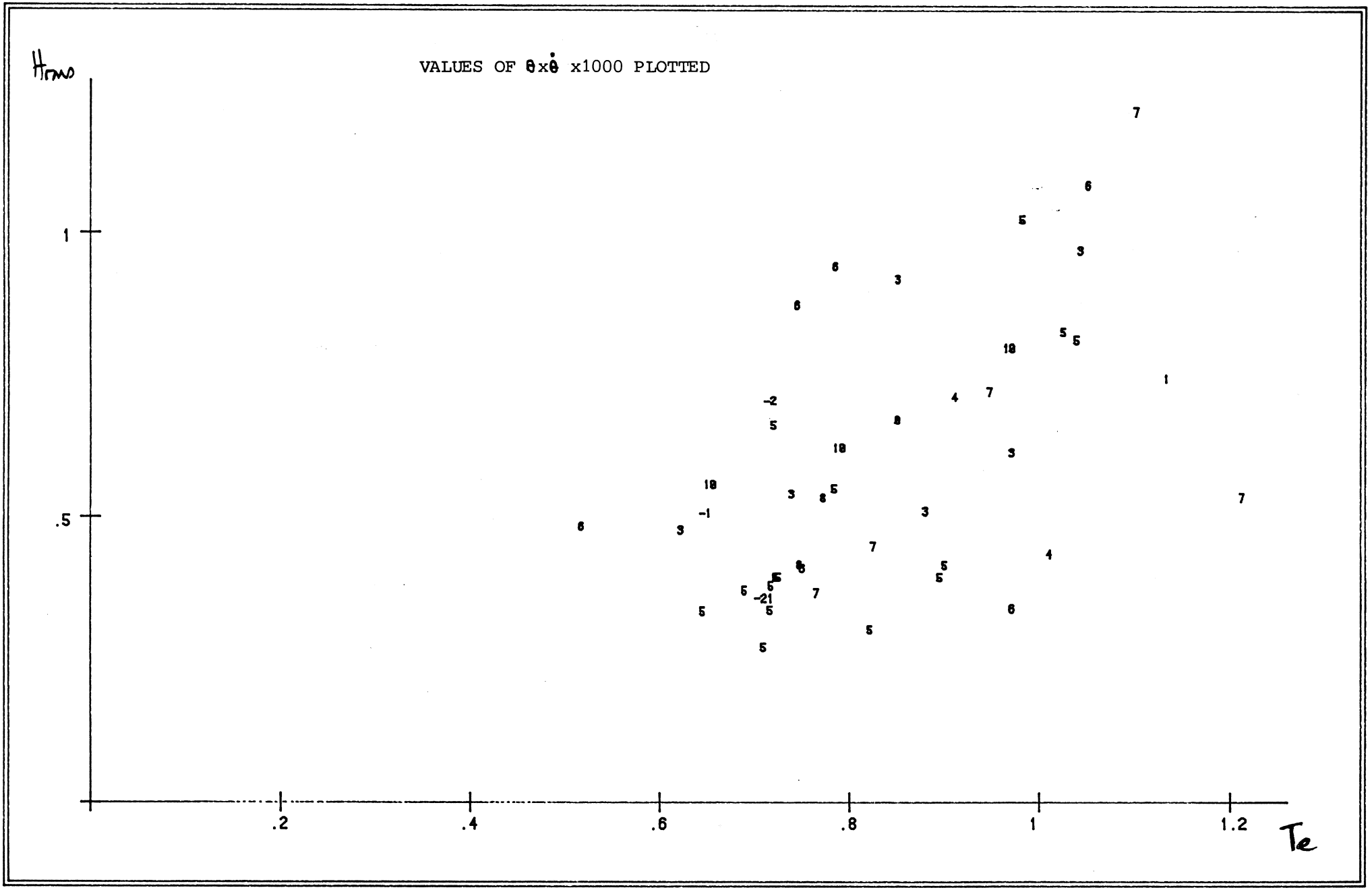

Figure D.17

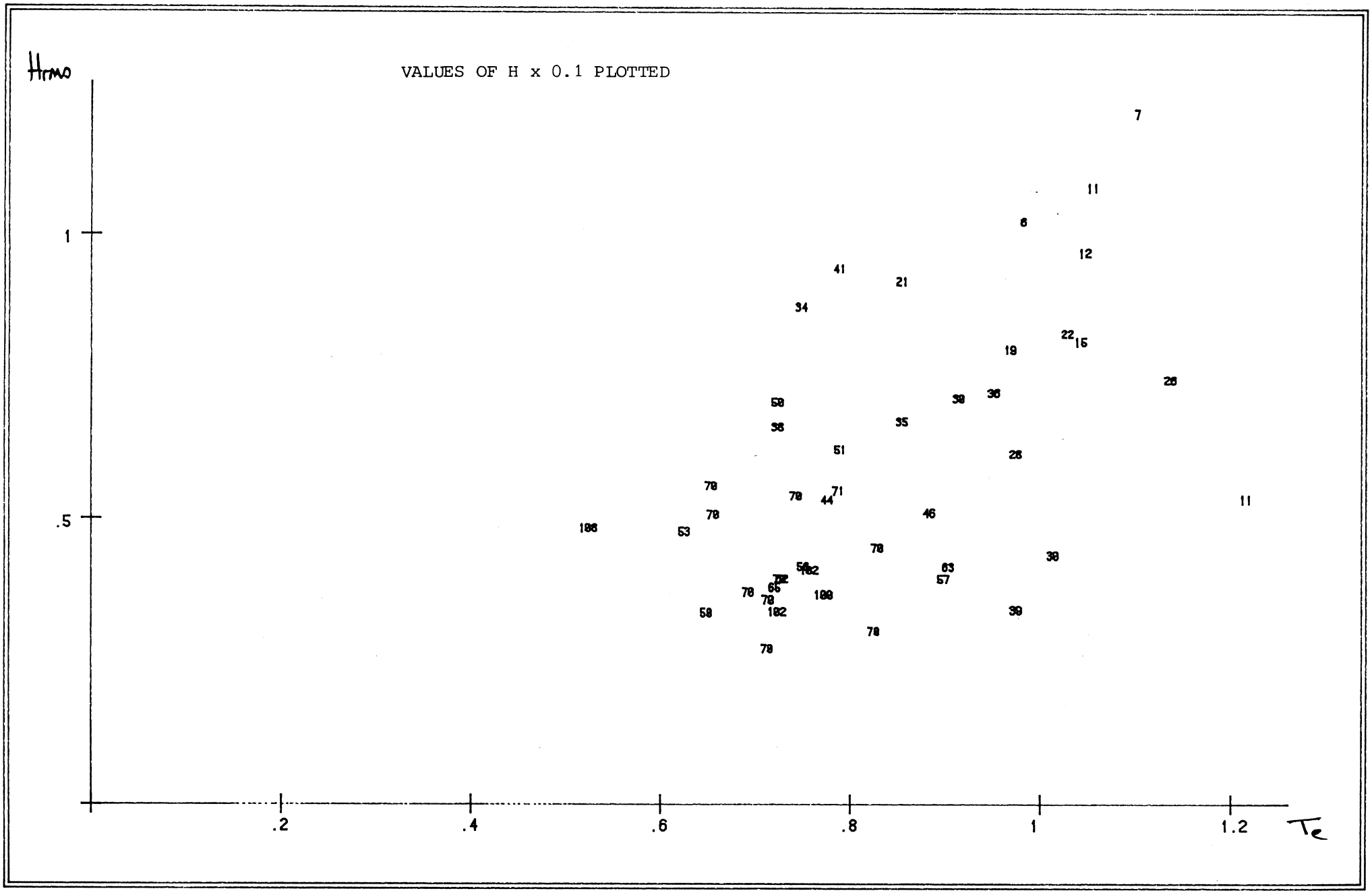

Figure D.18

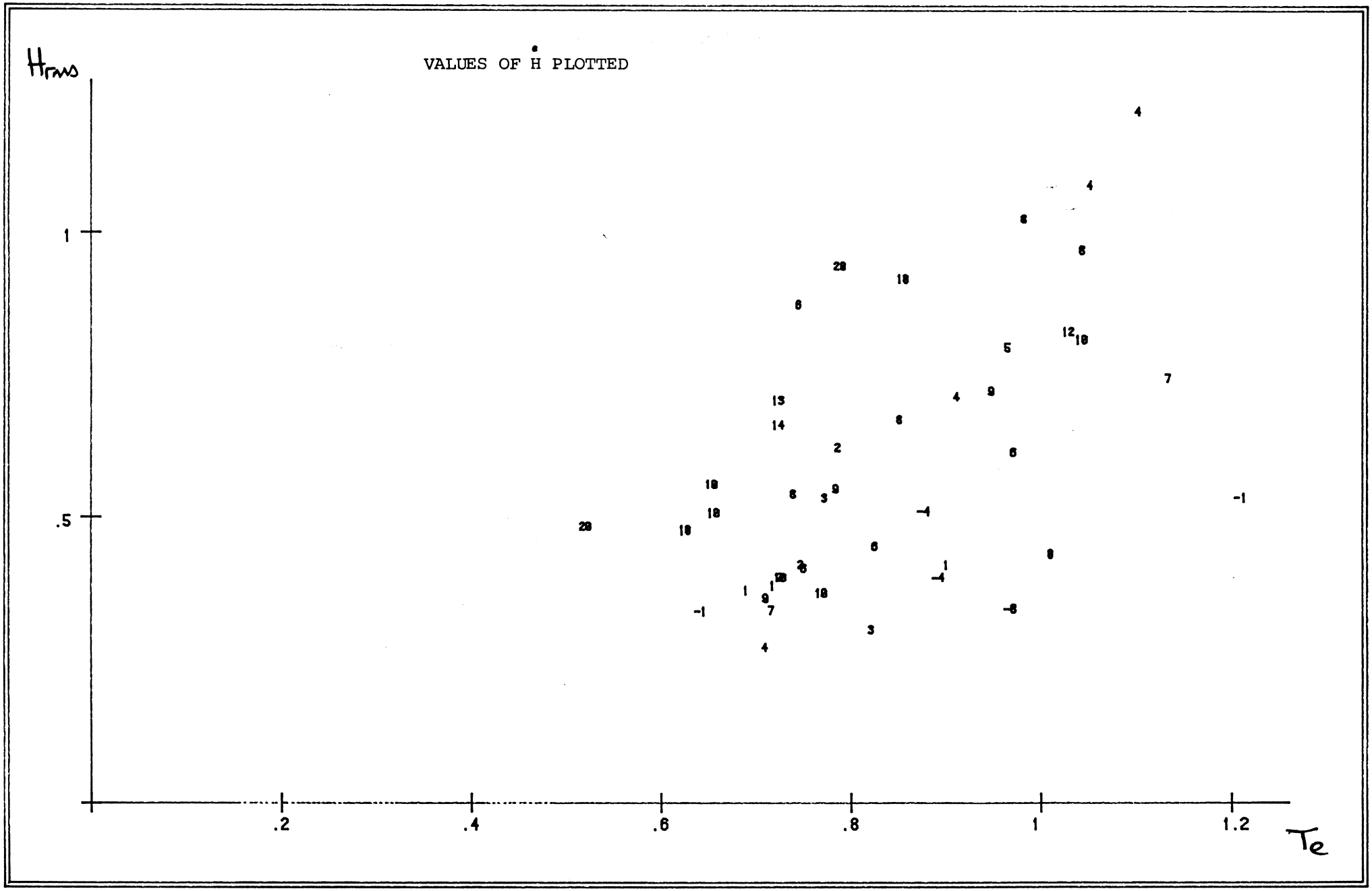

Figure D.19

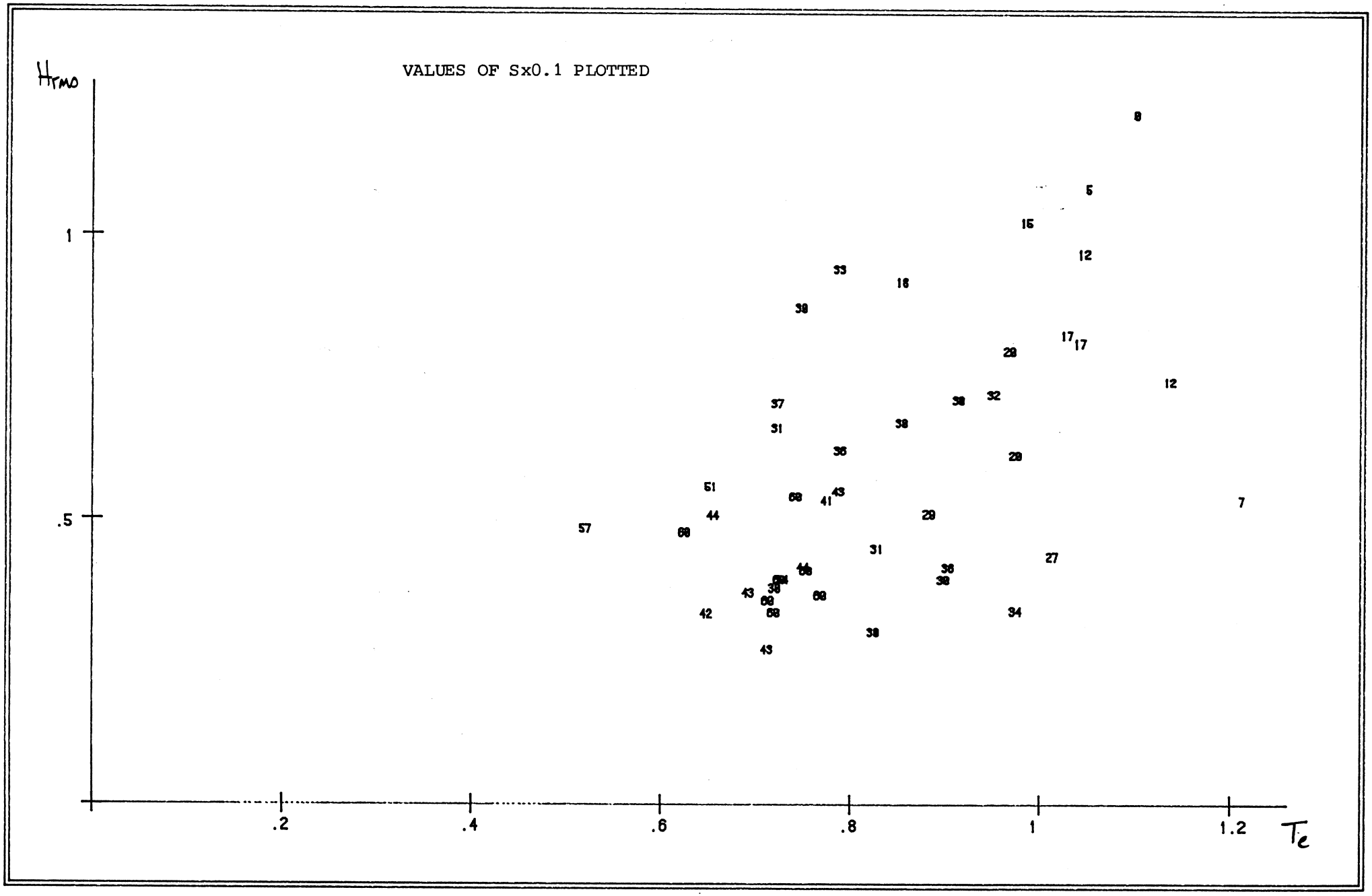

Figure D.20

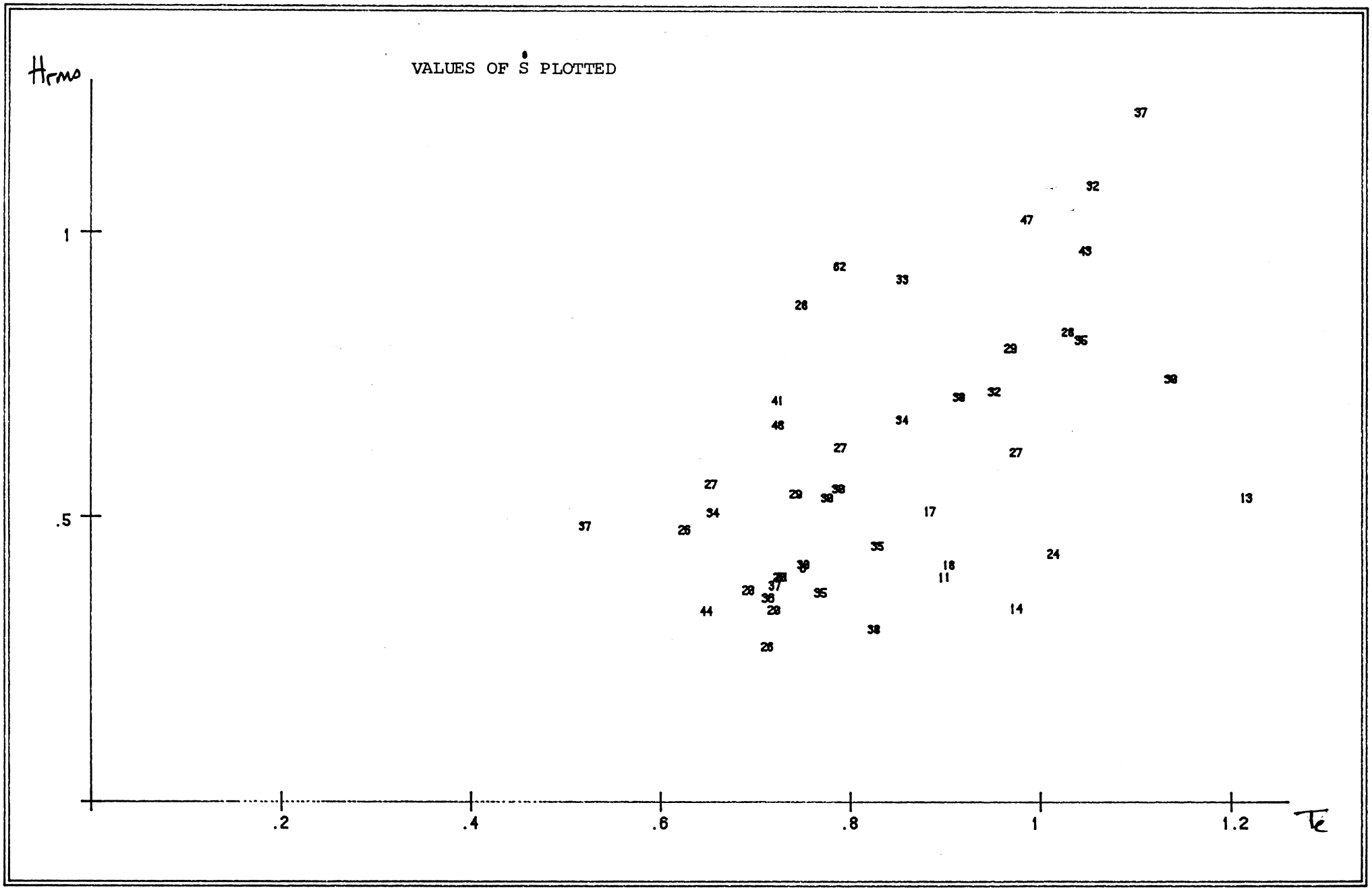

Figure D.21

Appendix E: 95% Confidence Intervals for Coefficient Values

Duck Spring Coefficient: DSC

$$\theta = \hat{\theta} \pm 2\left[V(\hat{\theta})\right]^{1/2} \qquad Nm/rad$$

where $\hat{\theta} = 0.0015 - 0.289\,T_e^2 + 0.179\,T_e H_{rms}$

and $V(\hat{\theta}) = 0.002 + 0.0048\,(T_e^2 - 1.528,\, T_e H_{rms} - 1.112) \begin{pmatrix} 0.287 & -0.345 \\ -0.345 & 0.468 \end{pmatrix} \begin{pmatrix} T_e^2 \\ T_e H_{rms} \end{pmatrix}$

Duck Damping Coefficient: DDC

$$\dot{\theta} = \hat{\dot{\theta}} \pm 2\left[V(\hat{\dot{\theta}})\right]^{1/2} \qquad Nm/rads^{-1}$$

where $\hat{\dot{\theta}} = 0.0772$

and $V(\hat{\dot{\theta}}) = 1.72 \times 10^{-4}$

Velocity Displacement Coefficient: VDC

$$\theta \times \dot{\theta} = f(\theta) = \hat{f}(\theta) \pm 2\left[V(\hat{f}(\theta))\right]^{1/2} \qquad N^2m^2/rad^2/s$$

where $\hat{f}(\theta) = 0.0045$

and $V(\hat{f}(\theta)) = 2.28 \times 10^{-5}$

Heave Spring Coefficient: HSC

$$H = \hat{H} \pm 2\left[V(\hat{H})\right]^{1/2} \qquad N/m$$

where $\hat{H} = 1.6 + 2656\,T_e - 484\,H_{ms} - 1967\,T_e^2$

and $V(\hat{H}) = 1007 + 22553\,(T_e - 1.722, H_{ms} - 1.244, T_e^2 - 1.528) \begin{pmatrix} 1.151 & -0.234 & -1.041 \\ -0.234 & 0.424 & -0.081 \\ -1.041 & -0.081 & 1.204 \end{pmatrix} \begin{pmatrix} T_e \\ H_{ms} \\ T_e^2 \end{pmatrix}$

Heave Damping Coefficient: HDC

$$\dot{H} = \hat{\dot{H}} \pm 2\left[V(\hat{\dot{H}})\right]^{1/2} \qquad N/m/s$$

where $\hat{\dot{H}} = 0.056 - 20.56\,T_e + 64.7\,H_{ms} - 35.7\,H_{ms}^2$

and $V(\hat{\dot{H}}) = 0.623 + 16.24\,(T_e - 1.722, H_{ms} - 1.244, H_{ms}^2 - 0.914) \begin{pmatrix} 0.860 & -1.97 & 1.08 \\ -1.97 & 4.96 & -2.96 \\ 1.08 & -2.96 & 1.93 \end{pmatrix} \begin{pmatrix} T_e \\ H_{ms} \\ H_{ms}^2 \end{pmatrix}$

Surge Spring Coefficient: SSC

$$S = \hat{S} \pm 2\left[V(\hat{S})\right]^{1/2} \qquad N/m$$

where $\hat{S} = 2.8 + 1529\,T_e - 1082\,T_e^2 - 278\,T_e H_{ms}$

and $V(\hat{S}) = 446 + 7648\,(T_e - 1.722, T_e^2 - 1.528, T_e H_{ms} - 1.112) \begin{pmatrix} 0.957 & -1.03 & 0.03 \\ -1.03 & 1.4 & -0.36 \\ 0.03 & -0.36 & 0.46 \end{pmatrix} \begin{pmatrix} T_e \\ T_e^2 \\ T_e H_{ms} \end{pmatrix}$

Surge Damping Coefficient: SDC

$$\dot{S} = \hat{\dot{S}} \pm 2\left[V(\hat{\dot{S}})\right]^{1/2} \qquad N/m/s$$

where $\hat{\dot{S}} = 0.32 + 59.7\,T_e + 27.3\,H_{mS} - 49.5\,T_e^2$

and $V(\hat{\dot{S}}) = 3.446 + 74\,(T_e - 1.722, H_{mS} - 1.244, T_e^2 - 1.528) \begin{pmatrix} 1.15 & -0.23 & -1.04 \\ -0.23 & 0.42 & -0.8 \\ -1.04 & -0.8 & 1.2 \end{pmatrix} \begin{pmatrix} T_e \\ H_{mS} \\ T_e^2 \end{pmatrix}$